Johnson S. C. LAM
81 Cabana Blvd
BENOWA WATERS
QLD 4217

27 October 1997

The Dean
Faculty of Engineering
University of Queensland
ST LUCIA 4067

Dear Sir,

In accordance and partial fulfillment of the requirements for the degree of Bachelor of Electrical and Electronics Engineering (Honours) at the University of Queensland, I hereby submit for your consideration this thesis titled: “A Steerable Planar Antenna System for Wireless LAN”.

Yours faithfully,

Johnson LAM

ACKNOWLEDGEMENTS

The author would like to express his total appreciation to his supervisor, Associate Professor M. E. Bialkowski, for his valuable advice and guidance on the project throughout the year, and the selection of such an interesting topic.

Thanks must also go to the numerous postgraduate students for their assistance and technical support for the thesis.

Many thanks to the lab supervisor Mr Ray Whitehead for his help and advice during this period, particular in relation to acquiring various equipments.

Last but not least, the author would like to extend his thanks to his family, especially his parents for their support and encouragement throughout the long years.

Johnson S. C. LAM

ABSTRACT

The thesis is concerned with the development of a planar quasi-optical amplifier antenna system for use in wireless local area networks (WLANs) at 10GHz. Its prime requirements are conformability and beam steering capability. Therefore, this thesis utilised the technology of microstrip antennas incorporated with a low-noise HEMT (High Electron Mobility Transistor) intended for X-band operation to design an active antenna array used in the reflection mode relay station.

The multi-layer aperture coupled feeding configuration is used for the design of microstrip antenna patch in an attempt to provide increased impedance bandwidth over conventional single layer structures. Indeed, from both the simulation and experiments, this theory has been proven correct. Compared to the typical bandwidth of single layer edge fed construction (generally 4-5%), the patch antenna in this thesis demonstrated a simulation bandwidth of 21.5% under the CAD software *Ensemble*, and obtained 17% from the tests of the experimental patch.

The use of millimeter wave frequency has the negative effect of low solid-state device power characteristics. Therefore, by utilising an array structure and employing the highly efficient technique of quasi-optical power combining, this thesis has demonstrated the capabilities of a 2x2 4-element array amplifier in areas of improved gain, directivity and beam steering.

The actual dimension of the 4-element array measures only 88.9mmx61mm (WxH), the experimental measurements show a gain of 27.021dB and derived from this, a patch gain of 5.5dB. Its radiation pattern provided a –3dB HPBW of 16° with major grating lobes of –3dB level at an offset of 31° and 58°.

Furthermore, the gain of 2-elements within the 4-element array was exactly 3dB down at 24.021dB, which demonstrates the 100% power combining efficiency of the quasi-optical power technique.

CONTENTS

List of Figures and Tables

CHAPTER 1

INTRODUCTION

1.1 INTRODUCTION

Today, the world lives in a completely dependent environment where the use of mobile telephones and other wireless data services are becoming essential in everyday routines. In particular, the field of wireless communications is experiencing unprecedented market growth, evident by the rapid increase in the size of cellular cordless telephone, paging, mobile data, and Wireless Local Area Network (WLAN) industries. This growth will become more apparent as the 21st century approaches, where the widespread deployment of wireless networks are going to revolutionise the concept of communication and information processing for business, professional, and private applications. Currently, there is an enormous shift in the computer industry toward integration of high performance distributed computing and portable devices in a mobile computing environment. This has led computer and telecommunication companies traditionally involved in wired services and product development, to rapidly invest in wireless communications to include mobile computing and networking features into laptop, palmtop, notepad, and other portable computing devices. Large corporations, playing the role of end-users, are also including wireless components in the infrastructure of their networks to extend the computational power of their networks to their field service personnel. Furthermore, military agencies are developing personal wireless devices for use in tactical environments, as well as portable devices providing extensive computational power for soldiers. All these factors reinforces the belief that the world of communications is experiencing a dramatic shift from a technology previously relied on wires to an era of networks largely based on wireless techniques.

1.2 MOTIVATION AND IMPORTANCE OF WORK

Within this communications revolution, even traditional wireless information networks, which include cordless cellular telephones, paging systems, mobile data networks and mobile satellite systems, have experienced enormous growth over the last decade, therefore the new concept of wireless LANs (WLANs) has emerged. WLAN is the direct result of an ever-increasing demand for portable information sharing in a wireless-networking environment from computer users. It facilitate ubiquitous, anytime, anywhere communications offering the user a degree of mobility never thought possible in a conventional LAN environment. A WLAN is a flexible on-premise data communication system implemented as an extension to, or as an alternative for, a wired LAN which substantially reduce the need for wired connections, hence making new applications possible. Although reliable links of high data-rates can be achieved using wired technologies, such as coaxial cable and optical fibre, WLAN has the unique advantage in providing a simple and cost effective solution when it comes to reconfiguration and upgrade, which conventional LAN finds very difficult and costly in a typical building environment. It is estimated that, for a new LAN installation consisting of software, hardware, and cabling, the investment in cabling alone can cost up to 40% of the installation [1.1]. Statistics have also shown that in 1990 alone, the total cost of relocating LAN terminals in the United States was US$5.6 billion, approximately half of the year's 12 billion dollar LAN maintenance market [1.2, 2.4]. Although WLAN is still at its early stage of development, achieving US sales of only US$57 million in 1993, it is rapidly growing with a projected US$900+ million in 1998 [1.3]. Furthermore, the Yankee Group, a market research firm, predicts a sixfold expansion of the US wireless LAN market by the year 2000, reaching more than US$1 billion in revenue [1.4]. These figures suggest the importance for many great engineers, computer science specialists, and multi-talented managers to rapidly educate themselves in an area of technologies with which they are somewhat or totally unfamiliar.

1.3 PREVIOUS DEVELOPMENT

Currently, wireless spread spectrum radio technique is the most widely used transmission technique for WLANs. It was initially developed by the military to avoid jamming and eavesdropping of the signal. This is done by spreading the signal over a range of frequencies, which consist of the Industrial, Scientific, and Medical (ISM) bands of the electromagnetic spectrum. The ISM band includes the frequency ranges at 902MHz to 928MHz and at 2.4GHz to 2.484GHz, which do not require a FCC (Federal Communications Commission of United States) license. The major drawback in this technology is the limited achievable data rate of only 2Mbps in the 902MHz band and 8Mbps in the 2.4GHz, as opposed to the 100Mbps obtainable in wired LAN structures [1.7]. The limited bandwidth and low data transfer rates of such commercial technologies presents a challenge for engineers to come up with innovative solutions in antenna designs for interfacing between wired and wireless portions of a system. As a result, there has been a push towards the millimetre wave frequencies to avoid the fierce competition for available spectrum in the congested RF band, which is mostly occupied by established commercial applications such as cellular networks and radio broadcasting. In Australia, the Radiophysics Division of CSIRO in Sydney plans to develop a millimetre wave WLAN system with transmission rates of up to 100Mbps [1.5]. One major obstacle with the use of millimetre wave frequency is the limited power achievable with solid state devices at such high frequency. A practical antenna system design proposed in [1.6] has provided a solution to this by utilising the highly efficient quasi-optical power combining technique. However, due to the narrow bandwidth nature of feeding mechanism (Edge Fed) used, the proposed design failed to provide attractive bandwidth desirable for WLAN applications. Consequently, this thesis aims to provide improvements over the existing design by employing aperture coupled feeding in an attempt to increase bandwidth.

1.4 OVERVIEW AND AIM OF THESIS

Chapter 2 will provide an overview of WLAN structures including some of the basic concepts, properties and requirements essential in such a system. It will include a discussion on technology options currently available for wireless LANs, which in effect forms the basis for development of this project.

Chapter 3 gives an introduction to microstrip antenna designs; it discusses the advantages and disadvantages associated with the various feeding mechanisms. A subsection of the chapter will be devoted to explore the concept of the highly efficient quasi-optical power combining technique for use in millimetre wave frequencies.

The theory and design method of the quasi-optical antenna amplifier is outlined in **Chapter 4**, it describes the procedures involved in designing and incorporating transmitting, receiving antennas with single active amplifier stage to form a unit cell. It includes the computer simulation results from various leading microwave CAD softwares. Furthermore, the design of a four-element array is also included to illustrate the practicality of the quasi-optical concept.

Chapter 5 consists of the experimental results, as well as a discussion on the suitability of such an antenna system for use in a practical WLAN environment. Conclusions, along with possible future development will be the main subject of **Chapter 6**.

REFERENCES

[1.1] Pahlavan, K. "Wireless Intraoffice Networks," *ACM Trans. Office Inf. Systerms, Vol. 6, No. 3, July 1988, pp. 277-302.*

[1.2] Marcus, M. J. "Regulatory Policy Considerations for Radio Local Area Networks," *Proc. of the IEEE workshop on Local Area Networks, Worcester, May 9-10, 1991, pp. 42-48.*

[1.3] Pozar D. M., "A Review of Aperture Coupled Microstrip Antennas", *University of Massachusetts at Amherst, May 1996.*

[1.4] "Introduction to Wireless LANs" *http://www.wlana.com/intro/introduction/* (accessed October 3, 1997).

[1.5] CSIRO Division of Radiophysics Sydney, Australia, "Australian Activities in Microwave Links for Wireless LANs", *IEEE MIT-S International Microwave Symposium Digest 1993, vol. 2, pp 677-680.*

[1.6] Wong C. H., "A Steerable Planar Antenna System for Wireless LAN", *University of Queensland, 1996.*

[1.7] "What is a Wireless LAN", *http://www.cis.ohio-state.edu/~jain/cis788/wireless_lan/* (accessed October 3, 1997)

CHAPTER 2

WIRELESS LAN SYSTEM

2.1 WIRELESS LAN *VS* LAN

Conventional local area network provides fast and reliable connection for desktop computer to share information via wire, coaxial cable and optical fibres, which involves costly installations. In recent years, the rapidly increasing market of portable personal computers has led to the creation of a new type of LAN, known as wireless LAN. The WLAN serves the same purpose as that of a wired or optical LAN, that is, to convey information among the devices attached to the LAN. However, with the lack of physical cabling to tie down the location of a node on a network, the network is much more flexible. As opposed to the large amount of labour required adding or moving the cabling in any other type of network, WLAN has offered a solution to overcome the difficulties associated with installing, maintaining and upgrading wired networks in typical building environments. With the use of wireless connections, it enables portable computers to retain its portability without sacrificing the advantages of being connected to a network. A graphical comparison between a wired and wireless LAN is shown in Figure 2.1.

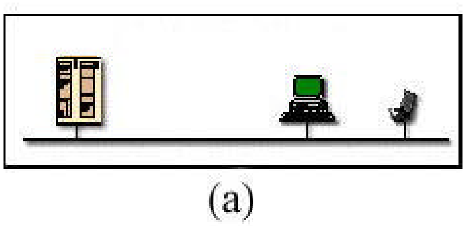

(a)

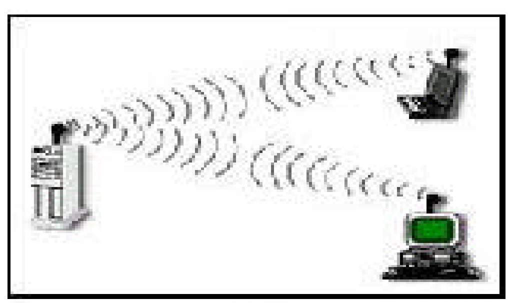

(b)

Fig 2.1. (a) Communication with server over standard LAN. (b) Communication with server over wireless LAN [2.1].

2.1.1 ADVANTAGES OF WLAN

With wireless LANs, users can access shared information without looking for a place to plug in, and network managers can set up or augment networks without installing or moving wires. In summary, wireless LANs offer the following productivity, convenience, and cost advantages over traditional wired LANs:

- *Mobility* – Wireless LAN systems can provide LAN users with access to real-time information anywhere in the access coverage, therefore supporting productivity and service opportunities not possible with wired LANs.
- *Installation Speed and Simplicity* – Installing a WLAN system can be fast and easy and can eliminate unnecessary setting up of cables through walls can ceilings.
- *Installation Flexibility* – Wireless technology allows the network to go where wire cannot reach.
- *Reduced Cost*-of-Ownership – While the initial investment required for WLAN hardware can be higher than the cost of wired LAN hardware, overall installation expenses and life-cycle costs can be significantly lower. Long-term cost benefits are greatest in dynamic environments requiring frequent movements, additions, and changes.
- *Scalability* – WLAN systems can be configured in a variety of topologies to meet the needs of specific applications and installations. Configurations are easily changed and range from peer-to-peer networks suitable for a small number of users to full infrastructure networks of thousands of users that allows roaming over a broad area.

2.1.2 DISADVANTAGES OF WLAN

Currently, the major drawbacks associated with wireless LAN are:

- *Slow throughput rate* – Factors that affect throughput include airwave congestion (number of users), propagation factors such as range and multipath, as well as the latency and bottlenecks on the wired portions of the WLAN. The common throughput rate for WLAN is about 1-10Mbps, whereas for a typical wired LAN, throughput rates of up to 100Mbps is possible [2.1]. Hence, a WLAN is suitable when dealing with text files or e-mail files, but if the use of multimedia graphics and sound is essential, conventional LAN setup is currently still the better choice.

- *Higher initial cost* – The initial cost for wireless LAN is about three times more expensive than that of cable LAN [2.2]. The infrastructure costs depend primarily on the number of access points deployed, where the number of necessary access points typically depends on the required coverage region and/or the number and type of users to be serviced. Studies have shown that a typical company can recoup the investment for a wireless LAN system in about one and a half years if a couple of moves are required during that period [2.2]. This amazingly quick capital recovery period is the result of two features offered by WLAN. Firstly, WLAN eliminates the direct costs and labour associated with installing and repairing the network. Secondly, the indirect costs of user downtime and administrative overhead are reduced during network relocation period.
- *Higher potential for electrical interference* – The unlicensed nature of radio-based WLAN means that other products transmitting energy in the same spectrum can potentially induce some level of interference. This interference is one of the factors that can cause degradation in throughput.
- *No set standard in industry* – At present time, there is still no wireless LAN standard that caters for the interoperability between equipments from different manufacturers. Although products from different vendors employing the same technology and implementation usually permit compatibility, there is no guarantee that the equipment will work together. However, the standardization of the IEEE 802.11 specification is current under way for transmission rates of 1 and 2 Mbps and is expected to be published in September 1997 [2.3]. The standard does not specify technology or implementation but simply specifications for the physical layer and Media Access Control (MAC) layer for manufacturers to build interoperable network equipment. In this respect, the WLAN industry is considered relatively primitive when compared to the more matured wired networks which have long conformed to specifications such as 802.3 (for CSMA/CD based Ethernet networks) or 802.5 (for token ring networks).

2.2 TECHNOLOGY OPTIONS

The achievable data rate is generally an important aspect in the design of a WLAN, and therefore the transmission channel characteristics and the application of signal processing techniques are important considerations. Access methods and network topologies used in WLANs are much the same from one system to another, but the transmission technologies are different. Efficient design of these systems requires evaluation of various transmission techniques and an understanding of the complexities of indoor electromagnetic propagation. Currently, WLANs employ the use of electromagnetic airwaves to establish wireless communication link between two points, and the competing approaches are either infrared radiation (IR) or radio (RF) waves in microwave or millimetre wave bands.

2.2.1 IR VERSUS RF

Infrared system carries data using high frequencies; its region of operation includes the lower portion of visible light in the electromagnetic spectrum and the shortest part of the microwave portion. Since IR has similar properties to light in that it cannot penetrate through opaque objects, its implementation is restricted to either direct line-of-sight (LOS) or diffuse technology. Inexpensive directed systems provide very limited range and are typically used for Personal Area Networks (PANs) but are occasionally used in specific WLAN applications. High performance directed IR is impractical for mobile users and is therefore used only to implement fixed subnetworks. Diffuse (or reflective) IR WLAN systems do not require LOS, but cells are limited to individual rooms. Currently, the most practical infrared system utilising diffuse IR technique have demonstrated raw transmission rates of up to 50Mbps in cells of few metres in radius [2.8]. However, the prospect of economically achieving reliable transmission rates over 10Mbps in a truly portable terminal is poor for the foreseeable future. This is primarily due to the difficulty in satisfying the high power requirements for acceptable signal to noise ratio when the diffusely received signals suffer delay spread and intersymbol interference (ISI) from multipath fading and dispersion, as well as environmental noise due to background light sources sharing the spectrum. Another common obstacle in IR links is its vulnerability towards human movements, which can only be avoided by positioning transmitter and receiver sufficiently high in order not to be obstructed. Weather conditions such as dust and fog also affect performance of IR optical systems. Despite the negative properties associated with infrared technology, the use of IR links can provide the following key advantages:

- Restricted optical transmission within a room resulting from low power level and LOS requirement offers greater data security.
- No need for a frequency assignment plan to avoid crosstalk, therefore eliminating FCC licensing and other regulation requirements.
- Well suited to environments with high degree of electromagnetic interference as it is not affected by electrical noise.
- Most importantly, it is cheaper than RF equipment.

On the other hand, although RF WLAN designs are generally more expensive and complex than IR alternatives, it offers the major advantage of full mobility required in a truly portable network. Radio Frequency also provides greater data throughput rate, which offers the ability to accommodate more users and multimedia traffic. Research [2.8] has shown that by moving towards millimetre wave frequencies, where the spectrum is sufficient to accommodate link speeds of hundreds of Mbps, a cellular approach with approximate range of 10 metres has demonstrated link rates of up to 185Mbps. Although RF provides coverage to areas without direct LOS to the transmitter, it suffers greatly from multipath signal reception, which induces significant destructive and intersymbol interference. Nonetheless, radio technology utilising millimetre wave has an enormous potential to succeed in indoor WLANs since there is virtually unlimited and unregulated spectrum available to offer near LAN performance. A comparison between IR and RF implementations is summarised in Table 2.1.

	Infrared (IR)	**Radio Frequency (RF)**
Cost	Low	High
Interference	Light spectrum (Sunlight, Florescent, Incandescent light), Human movement, Intersymbol (ISI)	Electromagnetic Radiation, Multipath Destructive, Intersymbol (ISI)
Coverage	LOS, Diffused	Non LOS
Mobility	Weak	Full
Regulation	No	License for μ & mm-waves
Performance	Low (10Mbps)	High (185Mbps)
Future Potential	Poor	Promising

Table 2.1. Comparisons between IR and RF

2.2.2 RF REQUIREMENTS

While the choice of radio technology is greatly dependent upon the application and cost factors. For WLAN use, the major requirements are frequency allocation, interference and multipath effects, and possible RF power outputs.

2.2.2.1 *FREQUENCY ALLOCATION*

The major and never-ending problem facing RF communications industry is the fundamental limitation on availability of frequency spectrum. Table 2.2 shows the most commonly used frequency bands for commercial WLAN applications. As can be seen, the frequency bands that may be considered for a wireless LAN system range from UHF to millimetre wavelengths. In particular, the unlicensed Industrial, Scientific, and Medical (ISM) bands at 900MHz, 2.4GHz and 5.7GHz presents a convenient solution common to WLANs. However, while ease of multi-user access can be gain from the unlicensed nature of these spectrums, performance degradation is inevitable when careless users cause unnecessary interference. Moreover, the limited achievable bandwidth associated with ISM bands also suggests a need to develop WLAN equipment using higher frequencies to enhance bandwidth required for future growth. As a result, a vast number of worldwide researches on high-speed WLANs have focused on millimetre wave frequencies to improve performance as well as to avoid the fierce competition for the small amount of unallocated spectrum in the lower microwave bands [2.7,2.8, 2.9,2.10].

FREQUENCY RANGE	DESCRIPTION
902-928MHz	Unlicensed spread spectrum band in the USA typical data rates of 9600-250,000bps
1850-1970MHz	New USA Personal Communication System (PCS) bands. Data rate is yet to be determined
1880-1990MHz	Digital European Cordless Telephone (DECT) systems 1.152Mbps gross data rate over the air
2400-2483MHz 2400-2483MHz 2471-2497MHz	Unlicensed spread spectrum band in USA Unlicensed spread spectrum band in Europe Unlicensed spread spectrum band in Japan Typical data rates of 9600bps-2Mbps
5.2GHz	10Mbps data rate HIPERLAN systems in Europe
5725-5850MHz	Unlicensed spread spectrum band in USA and Europe Typical data rates 5Mbps+
18-19GHz	Licensed band in USA used by Motorola Altair

Table 2.2. Most commonly used frequency band for WLAN applications

2.2.2.2 *MULTIPATH EFFECTS AND INTERFERENCE*

The major technical obstacle still to be overcome in the RF WLAN industry is the data rate limitation caused by the multipath characteristics of radio propagation. The multipath phenomenon is illustrated graphically in Figure 2.2. As the RF signal take multiple paths to reach the receiver from transmitter, it suffers many reflections causing the received signal to become stronger or weaker, therefore affecting data throughput. Such multipath and blockage results in intersymbol (ISI) and destructive (subtractive) interference that significantly limits available bandwidth and induce broadband fading noise. Hence, a robust modulation and error correction-coding scheme is essential to overcome ISI, while antenna diversity in the form of spatial or angle (beam steering) is imperative to combat destructive interference. Spatial diversity can be achieved by placing antennas a fraction of wavelength apart, which is feasible at millimetre wavelengths with the use of arrays. Accomplishing beam steering at these wavelengths is also quite practical by similar arraying format utilising the quasi-optical approach. Due to the unlicensed nature in some frequency spectrums, RF WLANs experiences another source interference. Because RF signals can penetrate walls, which enables open office environment, it also greatly increases the possibility of undesired interference from neighbouring WLANs transmitting energy in the same frequency spectrum. By moving towards the higher millimetre wave frequencies again provides a solution to this. At these frequencies, propagation is quasi-optical which has low penetration of walls, therefore signal transmission is confined within a room. At the same time, the wider bandwidth obtainable at such high frequencies from spectrum regulatory agencies will reduce the chance of overlapping frequency use from separate networks.

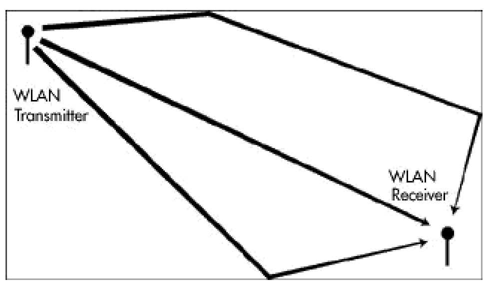

Fig 2.2. Radio Signals Travelling over Multiple Paths

2.2.2.3 *POSSIBLE RF POWER OUTPUTS*

The output power of wireless LAN systems is very low, especially in RF system because radio waves suffer rapid fading and significant multipath effects over distance. Since WLAN is intended for office environments, RF systems' low power output characteristics can be beneficial for safety reasons to produce acceptably low room radiation intensity in order to meet stringent government and industry safety regulations. At low frequency, the power output can easily be increased when necessary by well-established semiconductor technologies for long wavelength operation. However, when designing WLANs in the higher sub-millimetre and millimetre frequencies, such limited achievable power levels create some serious concerns. Within the millimetre wave band, some windows of frequencies suffer large atmospheric attenuation. Figure 2.3 shows this attenuation as a function of frequency in a typical atmosphere. Even though this helps to reduce interference with distant sources, it presents a challenge to achieve adequate power over operating range of the network. The major problem exists for poor solid-state device power capability at these high frequencies compared with those of longer wavelengths. A comparison of average power for several common active sources is shown in Figure 2.4. It can be seen that vacuum technology in general provides much greater output power than solid state devices. To overcome this, the power from many devices can be combined in an array by technique known as power combining. However, conventional circuit based combining approaches when used for millimetre wave designs often leads to bulky structures with high losses. Currently, the most promising method suitable for millimetre wave is quasi-optical solid state power combining where power is combined in free space with low loss. This technique will be discussed in chapter 3.

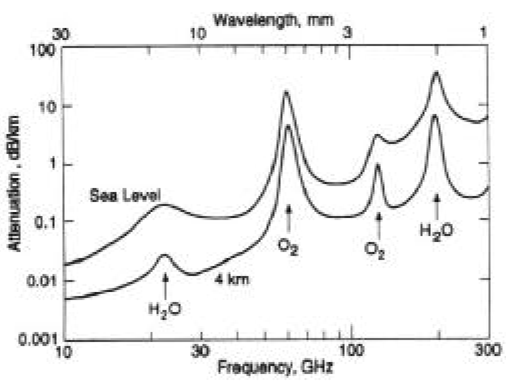

Fig 2.3. Typical atmospheric attenuation [3.5]

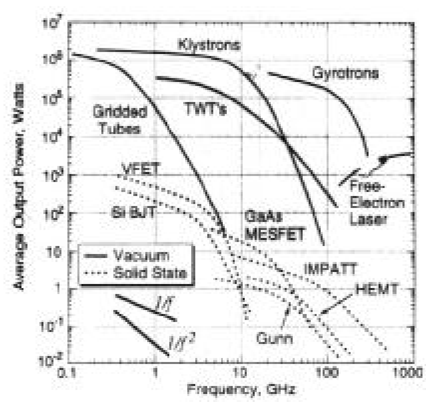

Fig 2.4. Power Handling capacity of various mm-wave sources [3.5]

2.3 WHY USE MILLIMETRE WAVES?

Currently, cellular communications, satellite TV, police radar, etc. are rapidly occupying the little available VHF, UHF, and low microwave region. As a result, there have been considerable advances in millimetre wave technologies for communication links to overcome this overcrowding of the lower microwave spectrum. With virtually unlimited and unregulated spectrum available at millimetre wave frequencies, systems promise large bandwidths and significant reduction in size and weight compared to existing microwave electromagnetic systems. Therefore, millimetre wave systems has strong potential for use in indoor wireless communications such as WLAN, or other environments subject to severe multipath distortion where the increased bandwidth is required to maintain robust communication links. The larger bandwidth available can also accommodate high data-rate systems to provide link speeds up to hundreds of Mbps where multiple fixed channels can be allocated using frequency division multiplexing in conjunction with spread spectrum techniques to help combat multipath fading. Furthermore, compact conformable antenna systems required by WLAN are made possible by the small component sizes associated with millimetre wavelengths. Other desirable features associated with millimetre wave includes

- Easier arraying to provide narrow beamwidth and electronic beam steering capabilities ideal for angular diversity used in WLANs.
- Low room radiation intensity required for safety of WLAN use.
- Signal confinement within operation zone to provide greater data security and reduced interference with distant sources.
- Small wavelength and high gain possibilities with narrow beamwidth are ideal for high angular resolution and low probability of intercept systems.

Currently, the main disadvantage of millimetre wave wireless LANs is the relatively high cost associated with the technology compared with that of lower frequency and optical systems. The most promising solution to cut down the cost appears to be the technique of monolithic integration [2.10], whereby manufacturing integrated circuit chips on a large scale, cost can be significantly reduced. Recent advances in the development of gallium arsenide (GaAs) based monolithic microwave integrated circuit (MMIC) extending its operation into millimetre wave suggests little doubt that monolithic millimetre wave integrated circuit (MMMIC) are the only cost effective solution to the future of millimetre wave technology [2.7].

Another major drawback associated millimetre wavelength designs is the limited power capability available from solid state devices at these high frequencies as described in the previous section. Nonetheless, this should not be of much concern as low power levels can be overcome by innovative power combining techniques such as quasi-optical power combining.

Table 2.3 shows a summary of millimetre wave features and common application systems.

<table>
<tr><th>Features</th><th>Advantages</th><th>Applications</th></tr>
<tr><td>Short Wavelength</td><td>Component downsizing
Narrow beamwidth
Low diffraction
Large Doppler shift</td><td rowspan="3">Satellite communication
Airplane communication
Mobile communication
Indoor communication
High speed communication
Doppler radar
Short pulse radar
Atmospheric sensor</td></tr>
<tr><td>Wide Bandwidth</td><td>Wide modulation band
Narrow pulse width
Multi-frequencies
Wide reception band</td></tr>
<tr><td>Propagation</td><td>High rectillnearity
Fog, water-vapour loss
Molecule absorption bands</td></tr>
</table>

Table 2.3. Millimetre wave features and applications

2.4 WLAN SYSTEM ARCHITECTURES

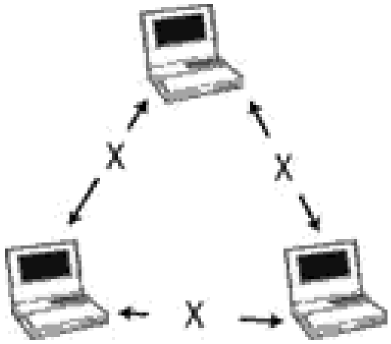

Fig 2.5. Independent WLAN [2.1]

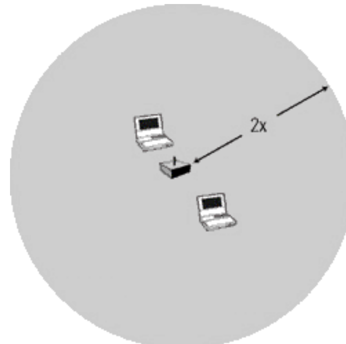

Fig 2.6. Independent WLAN with Access Point as Repeater to Extend Range [2.1]

The simplest form of a WLAN configuration is shown in Figure 2.5. In this setup, an independent network can be achieved anytime two or more PCs with wireless adapters are within range of each other. When a transmitter/receiver (transceiver) device, known as an Access Point is added to this network (Figure 2.6), it functions as a repeater, which effectively extends the range of the LAN by doubling the distance between the wireless PCs.

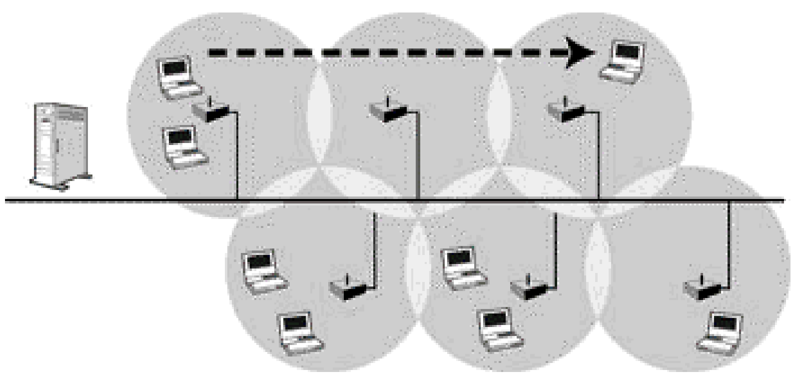

Fig 2.7. WLAN Infrastructure [2.1]

The infrastructure of a WLAN is presented in Figure 2.7, multiple access points are connected at a fixed position to the wired portion of the network via standard cables. The duty of the access point is to receive, buffer, and transmit data between the WLAN and the wired network infrastructure, as well as mediate communication between wireless network traffic in the immediate neighbourhood (ie. between access points). The antenna attached to the access point is usually mounted high, usually ceiling, but may be positioned anywhere that is practical to ensure desired radio coverage. However, the need for installation of cables through walls and ceilings to establish connections between base station and access points can be complicated and expensive. Such limitation is particularly apparent in large indoor areas such as warehouses, shopping malls, and stock exchange halls, where ceilings are typically not designed to provide a space for distribution of wiring. A new feeding approach presented in [2.5] has provided a solution to this problem by the introduction of no-wiring relay stations.

In this design, communication between the WLAN and wired network is still accomplished via the base station, however, signal is fed forward and backward by means of directional antennas on the base station and multi-beam antenna on each relay station. The multi-beam antenna serves the purpose of connecting each remote terminal within the cell to the network; hence a fast directional steerable antenna system is essential. The multi-path effects degrading throughput described previously can also be minimised with the use of such a steering scheme.

The difficulty now lies in devising a low cost antenna system to provide the fast steering required. A possible solution may be the use of phase shifter arrays [2.6]; however, the inclusion of relatively large phase shifters will significantly increase the antenna circuitry, which is inappropriate for the conformal nature of this project. Mechanical steering is also unacceptable as it is far too unresponsive compared to the travelling speeds of the signals. Therefore, the only feasible antenna option is the quasi-optical amplifier array, and its operation principle will be explain in Chapter 3.

Furthermore, because wireless communication is limited by the distance for a signal at given power output, cells known as microcells, similar to that of a micro-cellular mobile telephone system are employed to extend the range of wireless connectivity. This concept is illustrated graphically in Figure 2.8. At any point in time, a remote terminal is associated with only a single access point and its microcell's area of coverage. Individual microcells have small portions, which overlaps to allow continuous communication by handling low power signals and "hand off" users as they roam through a given geographic area.

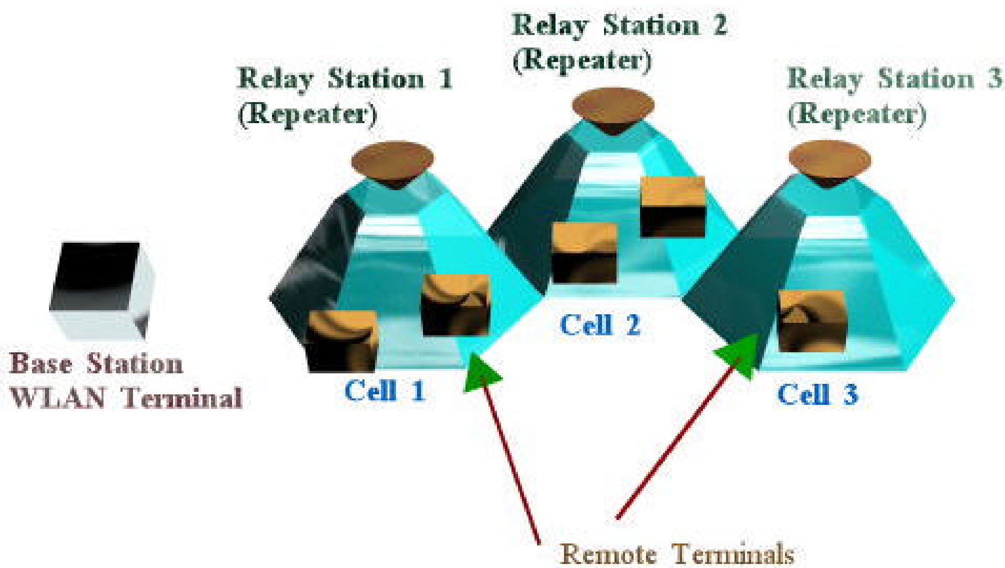

Fig 2.8. Typical cellular WLAN structure

In addition, it should be noted that the wireless part of the network cannot exist on its own, connections to external telecommunications network and between microcells can only be accomplished through the wired system via the base station. In fact, practical systems suggest a combination of wired and wireless LANs is likely to be adopted. In this, the machines that require relative mobility will be connected wirelessly, while the stations that are presumably permanent are connected through cable [2.7]. This approach not only take advantage of technology used in well-established LAN systems, it also permits high-capacity links with the use of optical systems. However, to ensure an overall high-speed system, the antenna used to interface between the wired and wireless parts of the network will require innovative solution, which is the objective of this thesis.

REFERENCES

[2.1] AMP Networking Communications Solutions, "What is Wireless LAN", *http://www.amp.com/networking/wireless/* (accessed October 3, 1997).

[2.2] "Weaknesses of Wireless LAN Technology", *http://www.weber.edu/ist/itfm/* (accessed October 3, 1997).

[2.3] Bernier, P., "Costs Slow Move To Wireless Data", *http://www.zdnet.com/intweek/daily/* (accessed October 3, 1997).

[2.4] Pahlavan K., Levesque A. H., "Wireless Information Networks", *Wiley New York, 1995.*

[2.5] Uehara K., Seki T., Kagoshima K., "New Indoor High-Speed Radio Communication System", *Asia Pacific Microwave Conference 1994, pp. 1035-1038.*

[2.6] Balanis C. A., "Antenna Theory: Analysis and Design, 2nd Edition", *John Wiley & Sons Inc., New York, 1997.*

[2.7] Parfitt A. J., Griffin D. W. and Cole P. H., "Monolithic Integrated Antenna Design for Millimetre-wave Wireless Local Area Network Systems", *Vol. 15, No. 2, Journal of Electrical and Electronics Engineering, Australia, June 1995, pp.137-143.*

[2.8] Skellern D. J., Lee L. H. C., McDermott T., Weste N. H. E., Dalton J., Graham J., Wong T. T., Myles A. F., Percival T. M. P., Ryan P. J., "A High-Speed Wireless LAN", *IEEE Micro, Jan/Feb 97, pp. 40-47.*

[2.9] Takimoto Y., Ihara T., "Research Activities on Millimeter Wave Indoor Communication Systems in Japan", *IEEE MTT-S International Microwave Symposium Digest 1993, vol. 1, pp. 673-676.*

[2.10] CSIRO Division of Radiophysics Sydney, Australia, "Australian Activities in Microwave Links for Wireless LANs", *IEEE MTT-S International Microwave Symposium Digest 1993, vol. 2, pp. 677-680.*

CHAPTER 3

ANTENNA SYSTEM FOR WIRELESS LAN

3.1 INTRODUCTION

In order to achieve a reliable, efficient, and high-speed WLAN, the antenna system used for interfacing between the wireless and the wired portions of the system must provide the following characteristics:

- Electronically beam steerable for quick switching between terminals, and to minimise multipath effects.
- Wide bandwidth to accommodate high throughput rates.
- Sufficient power capabilities to ensure adequate transmitted and received power levels maintaining constant robust communication link. However, radiated power intensity must not exceed safety limits.
- Narrow beamwidth to permit angle diversity usage.
- Small, lightweight, low profile and conformable to flat surfaces for suitable use in relay stations.
- Provides simple and flexible setup with minimum usage of wire connections to fixed structures such as walls and ceilings.
- Withstand interference from human movement and noise from other network sources.
- Suitable for use with higher millimetre wave frequencies.
- Low cost is essential.

This chapter describes an antenna system that may be used efficiently in RF wireless LAN operating at millimetre wave frequencies.

3.2 MICROSTRIP ANTENNAS

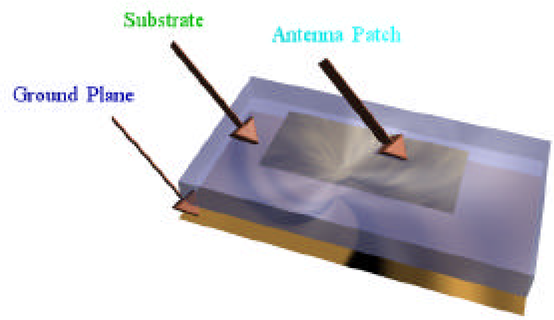

Fig 3.1. Microstrip antenna

Shown in Figure 3.1 is the simplest form of a microstrip antenna. It consists of a sandwich of two parallel conducting layer separated by a single thin low-loss insulating material, called dielectric substrate. The underside conduction functions as a ground plane, while the upper conductor operates as a radiating patch. If monolithic integration is employed, the upper layer will also include the feed network consisting of lumped components (resistors, capacitors, inductors, semiconductor, and ferrite devices) which can be added directly into the circuit.

Microstrip antennas radiate best at their resonant frequency, to achieve this resonant frequency, they are typically half a guided wavelength long and therefore the patch radiates a rather broad beam pattern.

The use of microstrip antennas can be considered as the ideal candidate for low-signal-level wireless LAN applications due to their numerous uniquely desired properties of:

- Low weight/volume/profile, thus easily incorporated into any package.
- Reduced cost with simple photolithography process eliminating the machining of complicated parts.
- Ease of installation and with the use flexible substrates, conformity onto flat or gently curved surfaces is made possible.

- Mass production capability.
- Since it appeared as a by-product of microstrip circuits, therefore, the design and realization takes advantage of well-established techniques developed for microstrip circuits and substrates.
- Low scattering cross section.
- Dual-frequency operation possibilities offering extensive flexibility to provide the finest construction of any shape.
- Direct integrability with microwave circuitry where feed lines and matching networks are fabricated simultaneously with the antenna structures to form microwave integrated circuits (MICs).
- Simple polarization (linear, circular) change by easy alterations of feed position.
- Compatibility with modular designs permits the fabrication process for simple series production of circuits and antennas. That is, lumped circuit and active solid state devices can be directly added to the antenna substrate board and combined with sections of transmission line.

Together with the rapidly increasing usage of the millimetre wave spectrum and the technological developments in millimetre wave components/circuitry, the requirement for new concepts in millimetre wave microstrip antenna has also expanded. Hence, significant advances have been made in the development and fabrication of microwave and millimetre wave monolithic circuits (MMICs and MMMICs) utilising microstrip antenna's ease of integration in the hope to provide an eventual low cost technology comparable with that of lower frequencies. In conjunction, it is optimistic that the use of integrated chips will lead to a more compact and reliable construction with reduced external connections.

However, like any developing technology, there are some limitations associated with the use of microstrip antennas, and can be listed as follows:

- Narrow bandwidth (Commonly 2-5% for single layer, 30% for multi-layer)
- Low gain (<18dB) and inherently low directivity.
- Higher loss.
- Half-plane radiation.
- Poor end-fire radiation performance.

- Low power-handling capability.
- Poor isolation between the feed and the radiating elements results in spurious radiation in the form of surface waves, which leads to high feed losses, poor radiation pattern and low efficiency.
- Difficulty to control sidelobe levels due to narrow bandwidth and spurious radiation.

Nonetheless, many of these limitations can be overcome by carefully choosing the substrate material and applying different design techniques for feeding, arrays and power combining. Such design considerations will be the subject of the next section.

3.2.1 *DESIGN CONSIDERATIONS*

The use of microstrip and printed circuit antennas at microwave and RF has matured somewhat, whereas at millimetre wave frequencies there remain many issues to be addressed with the need for further research and development. While it is convenient to use simple scaling procedures and to derive millimetre wave antennas from the microwave counterpart in the case of reflecting antennas or horns, slotted waveguide arrays. However, this approach is not always practical with microstrip antennas due to the reduction in size and tighter fabrication tolerances that arise. There are also severe limitations and problems due to substrate losses, feed requirements, and surface wave phenomena. Furthermore, the trend toward miniaturisation and use of integrated circuits, particularly utilising millimetre wave, does not support the use of scaled conventional antennas, as these would still be too large physically and difficult to integrate or conformably used. Thus special design considerations and procedures must be implemented if these antennas are to be used in the millimetre wave band.

3.2.1.1 SUBSTRATE MATERIALS

The dielectric substrate is the mechanical backbone of the microstrip antenna/circuit and ensures components are properly located and firmly in place. It also fulfills the electrical function of concentrating the electromagnetic fields and preventing unwanted radiation in circuits. Hence its permittivity and thickness governs microwave electrical characteristics of the antenna. Nonetheless, the dependence of dielectric constant on frequency is know to be reasonably low for frequencies up to 110GHz, where microstrip antennas are typically used [3.1].

The criteria for substrate selection for millimetre wave microstrip antenna is as follows:

I. Surface wave excitation possibility.
II. Effects of dispersion on the dielectric constant and loss tangent of the substrate.
III. Magnitude of copper loss and dielectric loss.
IV. Possibility of anisotropy in substrate.
V. The environmental effects of temperature, humidity, and aging.
VI. Mechanical requirements, such as ease of conformability, machineability, solderability, vibration effects on circuit dimensions, antenna weight, and ability to withstand gravitational forces.
VII. Most importantly, the cost.

From the above, only I, II, and III have particular significance to millimetre wave designs.

Due to the presence of an air-dielectric boundary in microstrip antenna, a large number of discrete surface wave modes are excited in the structure, with the number of modes generated being proportional to the thickness of the dielectric slab. Surface waves are undesirable effects that take up a portion of the signals energy, which leads to reduced signal amplitude and hence decrease antenna efficiency. Furthermore, surface waves presents spurious coupling between circuit and antenna elements, therefore degrading performance of microstrip filters as such interaction reduces the isolation in the stopbands. In array configurations, the high losses created by surface waves can significant affect the radiation pattern with very uncontrollable sidelobes and crosspolarization levels. Finally, due to resonance excited by surface waves arises the phenomenon known as blind spots which leads to particular directions in an array to neither transmit nor receiver. Thus, it can be seen that surface waves contribute mostly negative effects, so it must be significantly suppressed.

The undesirable effect of dispersion has significant dependence on dielectric constant and loss tangent, where the former decreases with frequency and the latter increases with frequency. Dispersion results in a variation of signal velocities within the frequency spectrum where the high frequency components travel faster than the lower frequency ones hence leading to severe distortions, particularly in broadband signals.

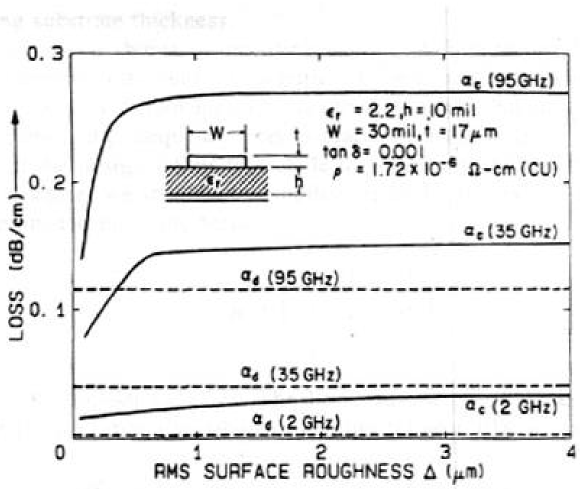

Fig 3.2. Effects of surface roughness and frequency on conductor and dielectric losses.

Figure 3.2 is the plot showing the dependence of conductor and dielectric losses on surface roughness and frequency. At high frequencies, the effect of surface roughness has a great influence on conductor loss. On the other hand, dielectric loss is relatively independent of surface roughness, but has a strong dependence on frequency. As a result, conductor loss is generally higher than that of dielectric. The dielectric loss can be minimised by choosing a low loss material having a moderately low dielectric constant, whereas copper loss, due to its strong dependence on frequency and surface roughness, it can only be reduced by choosing a substrate material which allows deposition of a mirrorlike conductor pattern. As a rule of thumb, surface roughness should be preserved at less than one-fifth of skin depth, and in millimetre wavelengths, is a roughness of approximately 0.1μm [3.1].

In general, in order to design a broadband microstrip antenna, the most effective method is to increase the substrate thickness and reduce its permittivity. However, an increase in thickness would lead to higher losses and the generation of surface waves, therefore microstrip lines can no longer be directly connected on the same substrate. At the same time, models derived from microstrip line theory are no longer valid, as they assume the use of thin substrates. Due to such limitations, it is essential to devise a microstrip antenna system that allows the optimization of radiating conditions for antenna element independent of providing a thin feed structure to favour propagation properties for the circuit. Clearly, a single layer design cannot achieve such conditions; therefore recent microstrip antenna development has move in the direction of multi-layer structures.

3.2.2 *FEEDING METHODS*

There are currently four main types of feeding methods for microstrip antennas, three of which utilises a single layer design, while aperture coupling by adopting multi-layer configuration, appears to have enormous potentials for improving on the impedance bandwidth obtainable in single layer designs. This section describes the various characteristics of each feeding method with their respective advantages and disadvantages.

3.2.2.1 EDGE FED

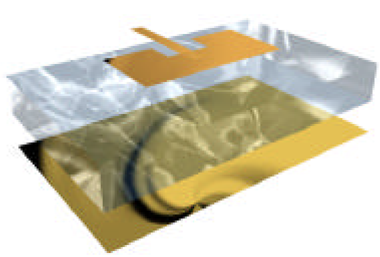

Fig 3.3. Edge fed

In the edge fed structure shown in figure 3-3, the feed line is attached directly to the radiating element, the structure take the advantage of being monolithic and provide good polarization characteristics. However, at the same time, it suffers from spurious radiation from feed network, and the need for an inset or transformer to match impedance.

3.2.2.2 PROBE FED

Probe feeding shown in figure 3.4 makes use of a probe through the ground plane passing the substrate to connect to the radiating patch. This can effectively provide impedance matching by means of probe location, which can also selectively excite additional modes, and when used with plated vias, multi-layer circuits can also be achieved. Nonetheless, it has the disadvantage of exciting cross polarization and the problem of highly inductive impedance when thick substrates are used.

Fig 3.4. Probe fed

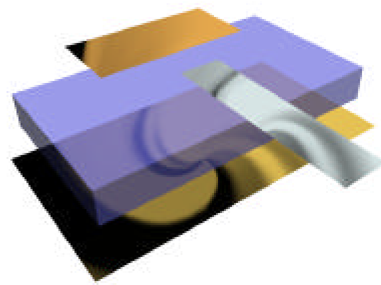

Fig 3.5. Proximity coupling

3.2.2.3 PROXIMITY COUPLED FED

The main advantage of proximity coupled fed shown in figure 3.5 is that there is no DC contact between feed and radiating patch exists, hence all coupling is achieved electromagnetically. This feeding configuration suffers from direct radiation of coupling region, as well as constraint in dimensional tolerance.

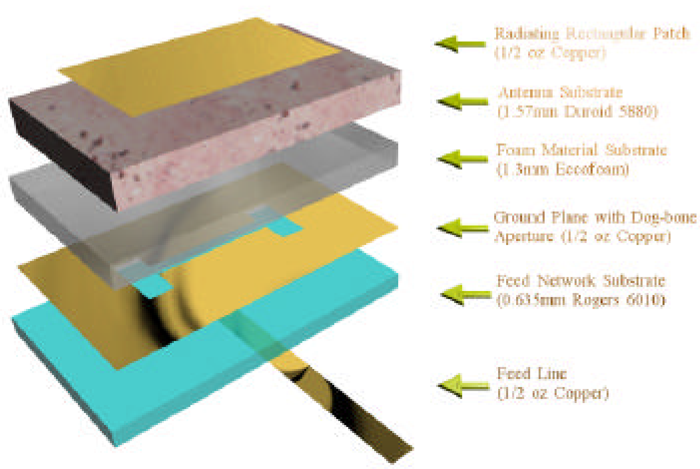

Fig 3.6. Aperture Coupling

3.2.2.4 APERTURE COUPLED FED

An improved version of aperture coupled fed microstrip antenna is shown in figure 3.6. With this feeding mechanism, coupling is accomplish through an aperture in the ground plane sandwiched between the radiating and feed network substrates. This geometry offers the ability of choosing radiator and feed substrates independently, as well as virtually eliminating spurious radiation from feed network without the need of via connectors as in probe fed. Generally, when a thick substrate is used for the radiating patch, there exist excess reactance where a tuning stub can be employed to adjust the inductive offset. At the same time, a double tuning effect can be accomplished by either bringing slot close to resonance or by introducing the stack configuration. The only major disadvantage of this is requirement of the complex multi-layer fabrication process, which often increase the cost.

3.2.3 EDGE, PROBE FED VS APERTURE COUPLED FED

Edge fed has the major limitation in that the feed line has to be negligible in size in comparison to the radiating patch to ensure minimum surface wave excitation on the common antenna/feed substrate. This makes edge fed configuration very inappropriate at high frequencies, where the resonant with of patch significantly decreases while feed remains essentially constant. On the other hand, probe fed does not have this problem, but the coaxial probe arrangement has an associated series reactance, which is dependent on the thickness and frequency, and creates more mismatching at high frequency ranges. Although shifting the location of the probe can reduce this mismatch, a shift would lead to a reduced bandwidth of the element. The key advantage that aperture coupling has over these single layer methods is the tremendous increase in bandwidth achievable through this feeding mechanism. While the bandwidth of single layer feeding structures such as edge and probe fed are limited to maximum of around 5%, aperture coupled elements can achieve up to 15% in standard configuration and up to an impressive 50% when stacked in multi-layers. The main reason for this improvement is the extra degrees of freedom offered by stub length and coupling aperture size. The bandwidth enhancement is also a direct result of the ability to independently choosing antenna and feed substrate, where an increase in height of patch layer is permitted without affecting feed layer. By selecting thick antenna substrate with low permittivity, surface wave excitation is better controlled, therefore providing flexibility with regard to eliminating scan blindness. The selection of low permittivity substrate increases the bandwidth and puts the scan blind point far from boresight, thus enhancing the maximum scan coverage sector. In contrary, by making feed substrate thin with high permittivity, spurious forward radiation can be greatly reduced causing it to be virtually isolated from the radiating element. Additionally, the use of common ground plane provides shielding to further suppresses the feed's forward radiation, at the same time isolating backward radiation from the antenna. This isolation provides better control of the cross-polarization level in arrays. Other benefits gained from the use of aperture coupling over single layer designs are:

- Eliminates the problems of reactance such as those associated with probe feeding.
- Considerable increases in substrate space for antenna elements and feed network.
- Feed circuitry layer can be separately integrated by modular approach leading to convenient integration for active arrays.

3.2.4 BANDWIDTH ENHANCEMENT TECHNIQUES FOR APERTURE COUPLED MICROSTRIP ANTENNAS (ACMA)

As previously stated, the most effective method in enhancing bandwidth of ACMA is by increasing the thickness of the antenna substrate. However, the thickness of the substrate can only be increased to a point where the generation of higher order surface wave modes and increase in feed losses becomes intolerable. Therefore, other techniques must be employed to further improve on the performance of ACMA.

In the previous section, it was described that the isolation of spurious radiation between radiator and feed circuit is greatly suppressed due to the ground plane used in ACMA. However, the use of large ground plane aperture for better coupling can have negative effects leading to an increase in both forward and backward spurious radiation. Therefore, to maintain good impedance bandwidth, it is undesirable to reduce slot size for achieving better isolation. Altering the shape of the slot to enlarged end-loaded shapes such as dog-bone, bow tie or H-shaped apertures provides a solution to this by significantly improving coupling without reducing isolation. This technique is ultilised in the design of figure 3.6.

It is apparent that the characteristics of microstrip antennas can be significantly improved by using multi-layer structures with thick substrates and low permittivity materials. Therefore, included in the design of figure 3.6 is the addition of low-dielectric-constant foam material instead of a thick antenna substrate. Because of its very low permittivity and remarkable mechanical properties, a significant reduction in the likelihood of producing surface wave is achieved, thus offering enhanced impedance bandwidth, as well as lower fabrication cost. The bandwidth is optimized through the adjustment of the foam thickness. Nevertheless, the addition of foam alters the impedance of the antenna, and since the input impedance is controlled by the size and position of the aperture, an increases in the aperture length is required to provide matching to 50Ω feed line, therefore leading to the undesirable effect of antenna back radiation. In this instance, the dog-bone geometry can be effectively applied to give same impedance bandwidth with appropriate reduction in aperture length.

3.3 ANTENNA ARRAY

In WLAN systems, an almost-omnidirectional antenna is required for the terminal to stay mobile, while for the relay station; a directional antenna system is preferred to achieve angle diversity. Since this project concerns with the design of the relay station antenna, narrow beam operation is required.

Individual planar elements suffer from limited power and are inherently low-directivity radiators with radiation patterns very similar to dipoles. To provide the desired characteristic of narrow beamwidth and increased directive gain required for electronic beam steering, two antennas (transmitter & receiver) can be combined in opposite polarization with an active stage for power gain to form a unit cell (figure 3.7), which is used to assemble an array structure. The purpose of the array is to arrange a number unit cells into a regular pattern so that the radiated fields combine along the desired direction and cancel out elsewhere. However, once arrayed, there are concerns with the radiation pattern suffering grating lobes for unit cell dimension that is larger than free space wavelength resulting in array element spacing larger than a wavelength. One solution to eliminate the grating lobes is by sub-arraying elements into a larger unit cell and setting the element and unit cell spacing so that the grating lobes of each sub-array is cancelled by the nulls of other. Therefore minimising possibilities of grating lobes by satisfying the criteria of achieving unit cell spacing $d<\lambda$ (wavelength).

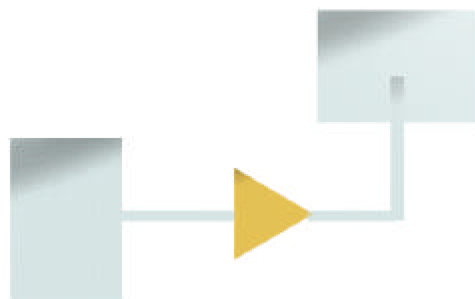

Fig 3.7. Amplifier antenna unit cell

In theory, the radiation pattern of the array is the original pattern of a patch multiplied by an array factor, which accounts for the geometrical positioning of the patches and the amplitudes and phases of the currents fed to them. However, in practice, patches interact with one another by phenomenon known as mutual coupling due to proximity with adjacent elements. With mutual coupling, currents are induced in surrounding patches and hence, provide coupling between the ports of the radiators (on the feed side) and additional radiation (on the antenna side). This causes significant effect to the radiation pattern and the input impedance depending on the location of the patch within the array, so careful arrangement of unit cells is essential to ensure a feasible design.

Commonly, arrays using single layered structures have their unit cells organized in a diamond shape to minimise space. However, the drawback with this arrangement is that only three elements can be realised in the unit cell. This problem is solved with the use of ACMA as radiating element [3.4]. Since separate antenna and feed network substrates are used, considerable space can be saved in the unit cell amplifier dimensions, which significantly helps to reduce development of grating lobes. The dimension of the array can be further reduced with the use of a single dual feed aperture coupled patch antenna instead of separate transmitting and receiving antenna. Nevertheless, a major problem with this approach is the poor isolation between the feeds, especially near resonance where significant feed coupling exists through aperture; this undesirable effect restricts the active stage gain due to the development of feedback oscillation.

3.4 QUASI-OPTICAL POWER COMBINING

As stated earlier, although millimetre wave frequency applications are advantageous for smaller and lighter antennas at a given directive gain compared to lower frequencies. There exists the major problem of poor solid-state device power capability at these high frequencies compared with those of longer wavelengths. To overcome the lack of power generated, the power from many devices in an array can be combined by technique known as Power combining.

Power combining techniques for microwave and millimetre wave frequency range can be separated into five main groups, Chip-level, Circuit-level (resonant cavity, non resonant), Spatial (Quasi-Optical belongs here), Multiple-level (combination of chip, circuit, and spatial), and other minority combiners [3.7,3.8].

Previously, classical cavity or conventional waveguide power combiners for use with microwave were limited in power, efficiency when applied at millimetre wave frequencies primarily due to:

- Higher conductor feeding losses.
- Tight constraints on manufacturing dimensions to within the same order wavelength so to achieve acceptable mode separation and to avoid multi-mode operation [1.6].

Quasi-optical power combiner, with the characteristics of forming array using large number of solid-state devices giving large linear dimension compared to wavelength, has provided a solution to the problem. Figure 3.8 contrasts between the methods of conventional corporate circuit transmission line feeder/combiner and spatial quasi-optical active array. It can be seen that distributed power is transmitted and received in free space without the need of feed/combining circuitries.

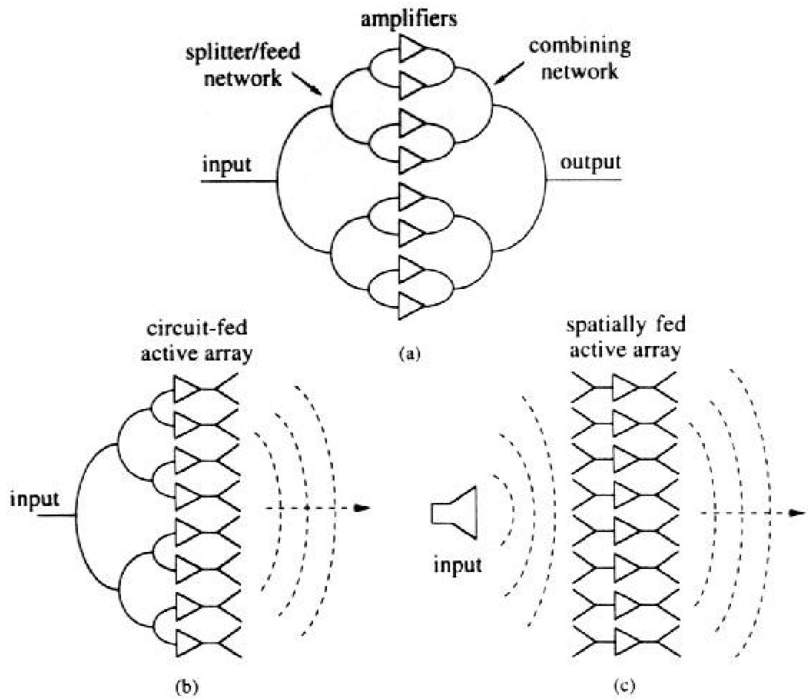

Fig 3.8. a) Circuit fed/combined array using corporate structure
b) Spatial combiner using circuit fed active array
c) Spatially fed/combined quasi-optical combiner [3.5]

Active quasi-optics promises great power increase from solid-state devices by combining the outputs of many devices with low loss in free space. In fact, quasi-optical technique is renowned for its ability to provide 100% power combining efficiency [1.6]. Quasi-optical amplifiers are multi-mode devices that can amplify beams at different angles, beams of different shapes, and even several beams simultaneously making them ideal for use with WLAN relay stations. A quasi-optical unit cell and 4-element planar amplifier antenna designed for operation at 10GHz is shown in figure 3.9 and 3.10, respectively.

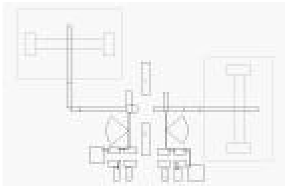

Fig 3.9. Quasi-optical unit cell amplifier

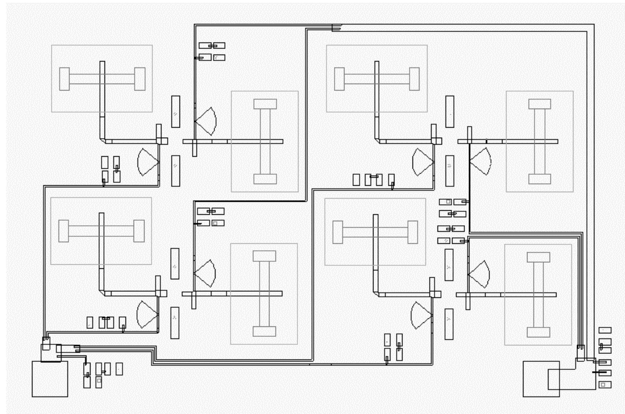

Fig 3.10. 4 element quasi-optical amplifier

Quasi-optical circuit operates by using distributed circuits effects, the same as that used in conventional microwave circuit, as well as using leakage and radiation from circuit as direct input/output ports. As a result, the open structure of quasi-optical combiner reduces the conductor losses by completely eliminating high loss feed networks. The quasi-optical combiner circuit is ideal for WLAN applications as it takes a planar geometry that can be easily integrated into MMMIC (monolithic millimetre wave integrated circuits). At the same instance, offering a compact system with single printed structure without the need for separate antenna, active stages and interconnecting lines. Further improvements can be achieved when individual quasi-optical unit cells are arranged in an array of appropriate size and spacing, some of the advantages provided are:

1) Increased output power due to signal combining in free space.
2) Increase gain due to higher directivity.
3) Frequency multiplication.
4) Angular diversity in arrays reduces fading in multi-paths.
5) Graceful degradation rather than catastrophic as devices fails because of intrinsic redundancy.

Finally, with the use of quasi-optical power combining, beam steering can be achieved [1.6,3.6] by activating specific array elements to provide directive and active gain in the desired direction.

REFERENCES

[3.1] Bhartia, P., “Millimeter-wave microstrip and printed circuit antennas”, *Boston, Mass.: Artech House, 1991.*

[3.2] Zurcher, J-F., “Broadband patch antennas”, *Boston, Mass.: Artech House, 1995.*

[3.3] Pozar, D. M., “A Review of Aperture Coupled Microstrip Antennas”, *University of Massachusetts at Amherst, May 1996.*

[3.4] Robinson A. and Bialkowski M. E., “Planar Amplifiers Using Edge-Fed And Aperture-Coupled Antennas For Wireless Communications”, *The University of Queensland, IWTS 97.*

[3.5] York R. A., Popovic Z. B., “Active and Quasi-Optical Arrays for Solid-State Power Combining”, *John Wiley & Sons, New York,1997.*

[3.6] Robinson A. Bialkowski M. E., “Planar Amplifier Elements For Active Reflectarrays”, *The University of Queensland, WARS 97.*

[3.7] Chang, K., Sun, C., “Millimeter-Wave Power Combining Techniques”, *Vol. MTT-31, No. 2, IEEE Transactions on microwave theory and techniques, Feb 1983, pp.91-107.*

[3.8] Russell K. J., “Microwave Power Combining Techniques”, *Vol. MTT-27, No. 5, IEEE Transactions on microwave theory and techniques, May 1979, pp.472-478.*

CHAPTER 4

THEORY AND DESIGN METHOD

4.1 INTRODUCTION

This chapter is concerned with the theory and methods the author used in designing a 10GHz planar quasi-optical amplifier antenna intended for operation in wireless LAN environment. This amplifier antenna is to be mounted on the reflection mode relay station mounted on the ceiling and it serves the purpose of interfacing between mobile PC terminals with the network via the base station. The power gain of the amplifier is achieved through the use a HEMT (High Electron Mobility Transistor) intended for operation in X-band (8-12.4GHz). The design of this antenna consists of three discrete stages, they are:

1) Antenna patch design
2) Single stage amplifier design
3) Quasi-optical array design

Each quasi-optical unit cell will consist of two antenna patches (one for receiving and one for transmitting), connected on input and output side of a single stage amplifier which is used to provide gain.

In the design process, various advance computer aided drawing and simulation softwares were used. First, the design dimensions of the antenna patch were optimized to 10GHz according to simulations under the *Ensemble* produced by Boulder Microwave Technologies. Then for the single stage amplifier, designed matching circuits were simulated under *PUFF* to ensure feasibility and adjustments to the circuits were made where appropriate. Next, the DC-biasing circuitry were drawn together with finalised matching circuit in *HP-EEsof Touchstone (Series IV)* produced by Hewlett Packard, and simulated. *Touchstone* was then used to perform optimization on various circuit parameters; once accomplished *Touchstone layout* generated the layout of the unit cell for fabrication. At last, *Touchstone Layout* was again employed to arrange the unit cell into a 2x2 array and fabrication mask generated. An important note to be aware of is that external microstrip feed line connections for both antenna patch and amplifier are design on 50Ω impedance to eliminate the need for extra matching circuitry when combining into an unit cell, and ultimately the 2 x2 array.

4.2 ANTENNA PATCH DESIGN

The aim of this thesis is that to use aperture coupled feeding mechanism for increasing the impedance bandwidth on previous design utilising edge fed configuration. As described in chapter 3, this is due to the flexibility offered by multi-layer structure, which provides independent substrate selection for antenna and feed network. Therefore, choosing the ideal substrate is crucial for maximum performance and substrates used for this design are listed in Table 4.1 along with their respective permittivity and thickness.

LAYER	SUBSTRATE NAME	PERMITTIVITY	THICKNESS
ANTENNA	Rogers Duroid 5880	2.2	1.57mm
FOAM SPACER	Eccofoam	1.03	1.3mm
FEED	Rogers Duroid 6010	10.2	0.635mm

Table 4.1. Substrates used for antenna design

With the above parameters entered into *Ensemble*'s database, design process can begin on determining various dimensions to provide operation at 10GHz. For ACMA, different trends can be realised with variation in a number of material and dimensional parameters, and these can be summarised in Table 4.2.

By altering the various dimensional parameters, the simulations for the s-parameter S_{11} (input reflection coefficient) can be obtained in different forms of plots. These plots are:

1) Input return loss on dB log scale.
2) Voltage stand wave ratio (VSWR).

3) Smith chart with S_{11} impedance locus.

LEVEL	PARAMETER	TREND
ANTENNA	Antenna dielectric constant	Affects bandwidth and radiation efficiency, lower it is, wider the bandwidth
	Antenna substrate thickness	Affects bandwidth and coupling level, thick it is, less coupling for a given aperture size
	Patch Length (L_p)	Determines the resonant frequency
	Patch Width (W_p)	Affects the resonant resistance, wider it is, lower resistance. Should avoid square path to reduce cross-polarization
	Patch position relative to aperture	Max coupling centred over slot. Move relative to slot in H-dir has little effect, while move towards E-dir will decrease coupling
GROUND PLANE	Aperture Length (L_a)	Determines coupling level, and back radiation level, therefore made no longer than required for impedance matching
	Aperture Width (W_a)	Affects coupling level to a less degree compared to length, ratio of typically 1/10
FEED	Feed dielectric constant	Select for good circuit qualities, range 2-10
	Feed substrate thickness	Thinner has less spurious radiation from feed, but higher loss, compromise bet 0.01-0.02λ
	Feed Line Width (W_f)	Control characteristic impedance and coupling to slot, thinner couple more strong
	Feed position relative to aperture	Max coupling with feed line right angle to slot. Skew feed from slot reduces coupling, as will positioning feed towards slot edge
	Tuning stub length (L_s)	Tunes excess reactance, typically slightly less than $\lambda_g/4$ in length, shortening stub will move impedance locus in capacitive dir on Smith Char, lengthening will move towards inductive

Table 4.2. Effects on variation of design parameters

Through examining the responses of these graphs, appropriate adjustments were made to the antenna design in order to obtain a 50Ω match with resonant frequency at 10GHz. A good result is determined by meeting the eventual goal of:

1) Obtaining maximum negative dB value at resonant frequency on input return loss plot and having as much of the spectrum under –10dB as possible to achieve good bandwidth.
2) Similarly for VSWR plot, a minimum must be achieved at resonant frequency and having as much of the spectrum below 2 as possible.
3) The point of the locus representing 10GHz in the Smith chart should run through the centre and intersecting the constant VSWR circle of 1.

The final design layout of the ACMA is shown in Figure 4.1. The key parameters to note in this design are:

1) The patch length of 9mm since it is the major determining factor of 10GHz resonant frequency.
2) The tuning stub length of 1.8mm as it tunes the excess reactance.
3) The aperture area as it has the greatest influence on the level of coupling between feed and radiator.

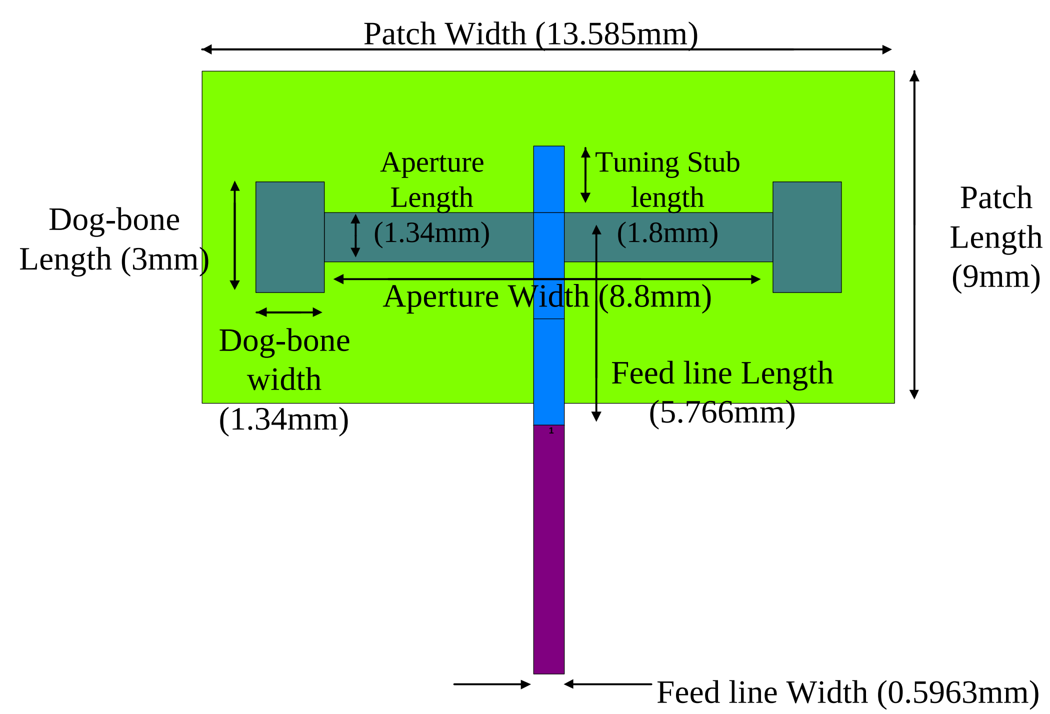

Fig 4.1. ACMA patch design layout

The simulated results of input return loss, VSWR, and Smith Charts are given in Figure 4.2, 4.3, and 4.4, respectively.

The figure of merit for input return loss and VSWR in figure 4.2, and 4.3 is the percent of impedance bandwidth achieved, and they are determined by the following:

1) For the S_{11} input return loss plot, the region of frequency that lies below –10dB divided by the resonant frequency is the percent impedance bandwidths obtained.
2) Likewise, the same percentage should be obtained for the region of frequency enclosed by the intersection points at VSWR of 2.

The equation is therefore given by

$$PercentBW = \frac{f_{hi} - f_{lo}}{f_o} \times 100\% \qquad (4.1)$$

where f_{hi} and f_{lo} represents the intersection frequencies, and f_o being the resonant frequency.

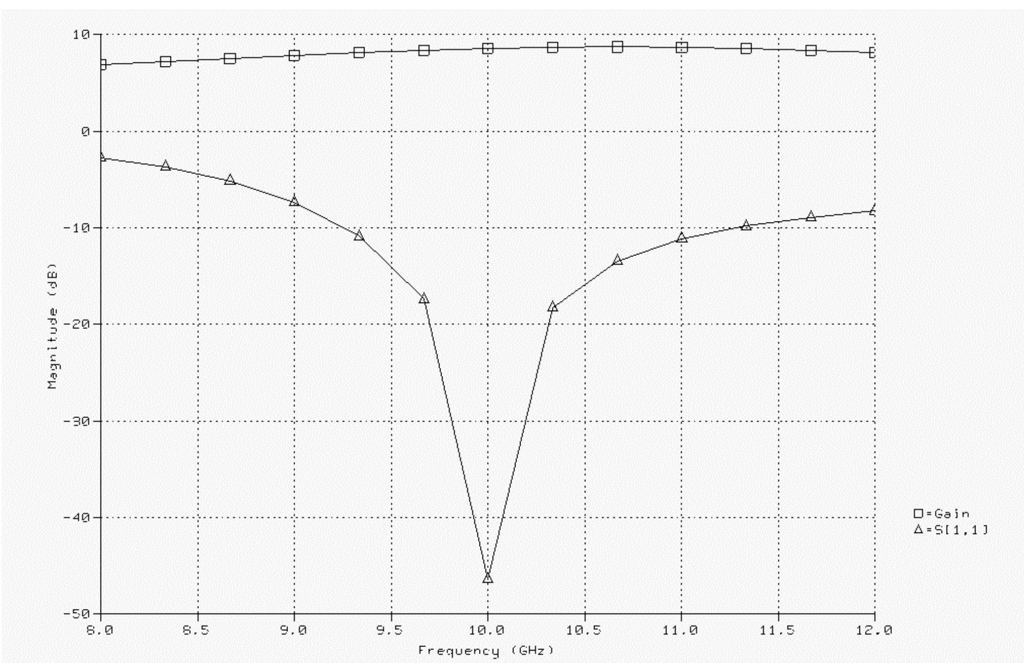

Fig 4.2. S_{11} input return loss plot for ACMA

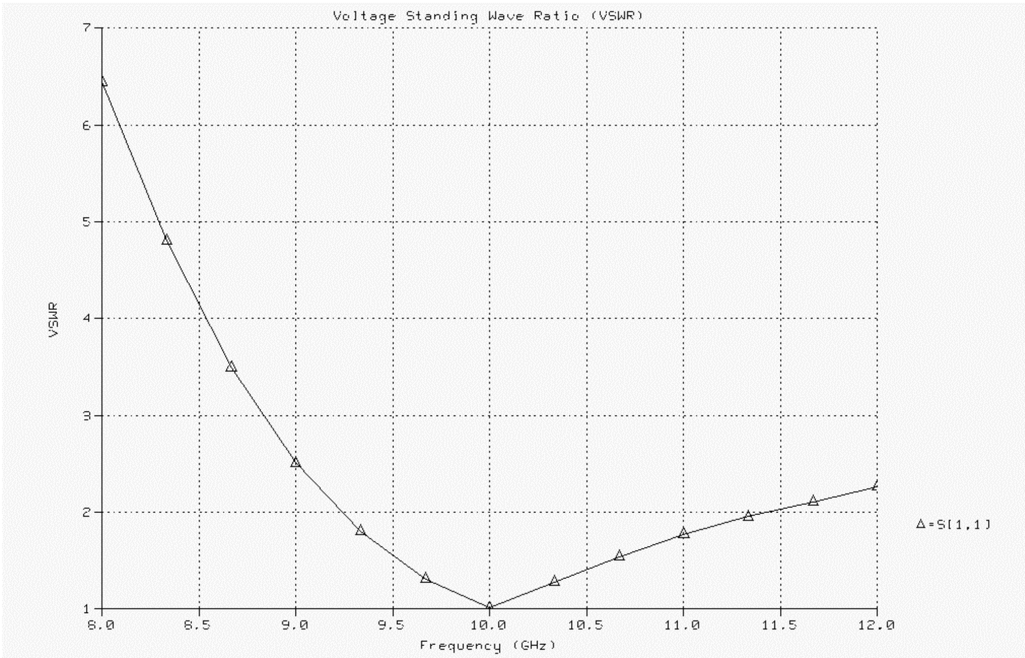

Fig 4.3. S_{11} voltage standing wave ratio plot for ACMA

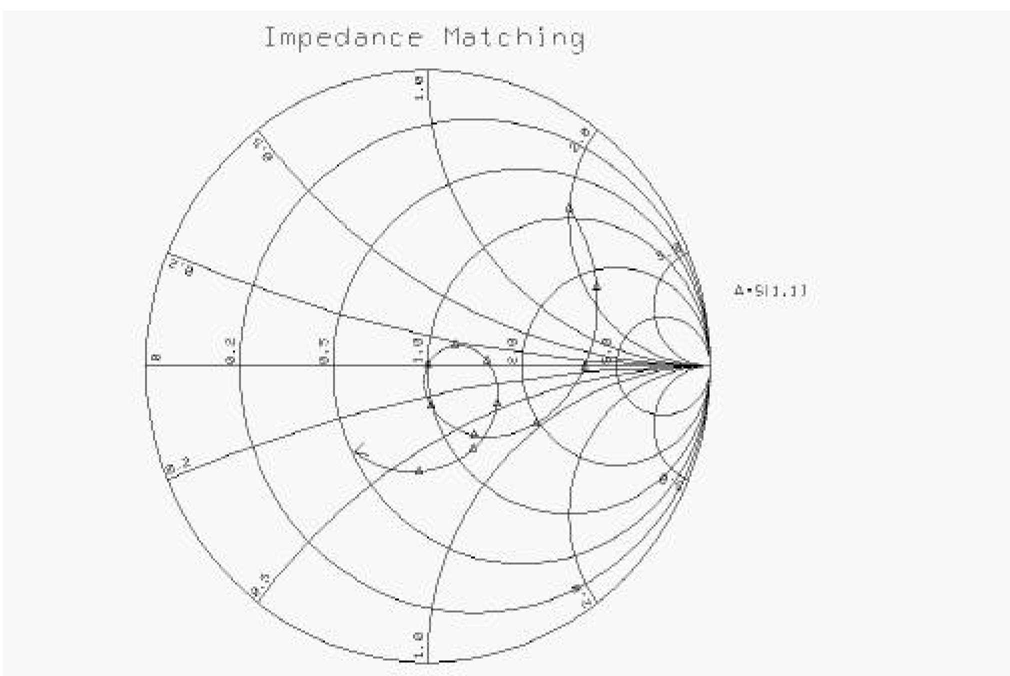

Fig 4.4. S_{11} Smith Chart for ACMA

From the simulations, the antenna patch demonstrates an achievable impedance bandwidth of 21.5% with an input return loss of –47dB at its resonant frequency, this is a good indication of a well matched, correctly dimensioned patch design. Furthermore, the designed 50Ω feed line enables direct connection with single stage amplifier designed with the same characteristic impedance.

4.3 SINGLE STAGE AMPLIFIER DESIGN

The procedures involved with the design of a single stage amplifier are:

1) Stability.
2) Maximal Transducer Power Gain.
3) Input and Output Matching Circuits.
4) DC Bias.

4.3.1 Stability

The stability of an amplifier is very important consideration in microwave circuit designs. The characteristic of the amplifier is determined by its S-parameters. With the use of the S parameters, the synthesized source, and the load impedances, the circuit's resistance to oscillation can be determined. Figure 4.5 shows block diagram of a single stage amplifier circuit with matching networks and reflection coefficients at various points.

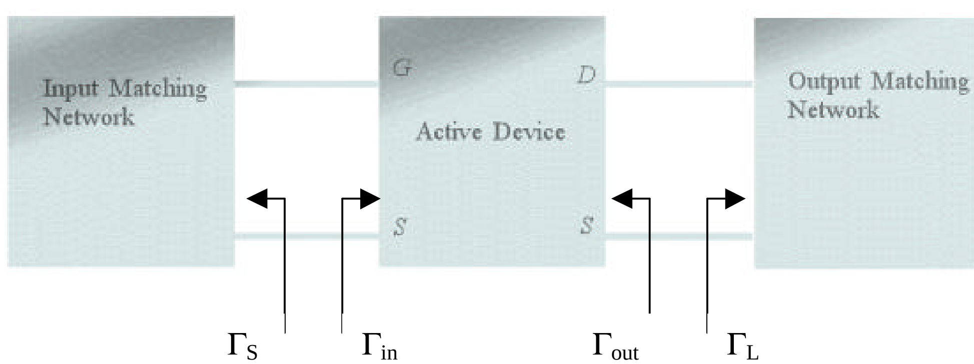

Fig 4.5. Block diagram of single stage amplifier circuit with matching networks

Oscillations are possible in a two-port network if either the input or output port, or both have negative resistance or when either $|\Gamma_{in}| > 1$ or $|\Gamma_{out}| > 1$. This occurs if $|S_{11}|$ or $|S_{22}|$ are greater than unity for a unilateral case ($|S_{12}| = 0$). Nevertheless, an amplifier with negative resistance might still be stable.

To calculate stability, the S-parameters provided by manufacturer's data sheets on the *Mitsubishi packaged low noise MGF1302 HEMT* are used. These data sheets can be found in Appendix A.

For an unconditionally stable microwave transistor amplifier, the magnitudes of S_{11}, S_{22}, Γ_{in}, and Γ_{out} must be less than unity, while the following requirements for stability factor (K) and the determinant of the scattering matrix (Δ) must also be satisfied.

$$K = \frac{1+|\Delta|^2 - |S_{11}|^2 - |S_{22}|^2}{2|S_{12}S_{21}|} > 1, \tag{4.2}$$

$$|\Delta| = |S_{11}S_{22} - S_{12}S_{21}| < 1 \tag{4.3}$$

As a result, the stability circles can be plotted directly on a Smith Chart which separates the output or input planes into stable and potentially unstable regions. A stability circle plotted on the output plane indicates the values of all loads that provide negative real input impedance (ie. $|\Gamma_{in}| > 1$), thereby causing the circuit to oscillate. Similarly, a stability circle plotted on the input plane indicates the values of all loads that provide negative real output impedance (ie. $|\Gamma_{out}| > 1$), and again causing oscillation. The regions of instability occur within the circles whose centres and radii are expresses by:

$$c_s\,(centre\,of\;\Gamma_s\;circle) = \frac{|C_s^*|}{\left||S_{11}|^2 - |\Delta|^2\right|} \tag{4.4}$$

$$c_L(centre\,of\ \Gamma_L\ circle) = \frac{|C_L^*|}{\left||S_{22}|^2 - |\Delta|^2\right|} \tag{4.5}$$

$$r_s(radius\,of\ \Gamma_s\ circle) = \frac{|S_{12}S_{21}|}{\left||S_{11}|^2 - |\Delta|^2\right|} \tag{4.6}$$

$$r_L(radius\,of\ \Gamma_L\ circle) = \frac{|S_{12}S_{21}|}{\left||S_{22}|^2 - |\Delta|^2\right|} \tag{4.7}$$

where

$$C_s = S_{11} - \Delta S_{22}^* \tag{4.8}$$
$$C_L = S_{22} - \Delta S_{11}^* \tag{4.9}$$

In summary, for unconditional stability any passive source and load impedance in a two-port network must produce the stability circles completely outside the Smith chart. However, if either of the stability circles overlap with the Smith Chart, the stability of the system is conditional.

Shown in figure 4.6 is the complete schematics of the single stage amplifier, its Smith chart simulation (figure 4.7) shows that the stability circles lies (denoted by square and circle) completely outside the Smith Chart, therefore, the circuit used is unconditionally stable within its frequency of operation in X-band. The chart also includes constant gain circles, which will be focus of next section.

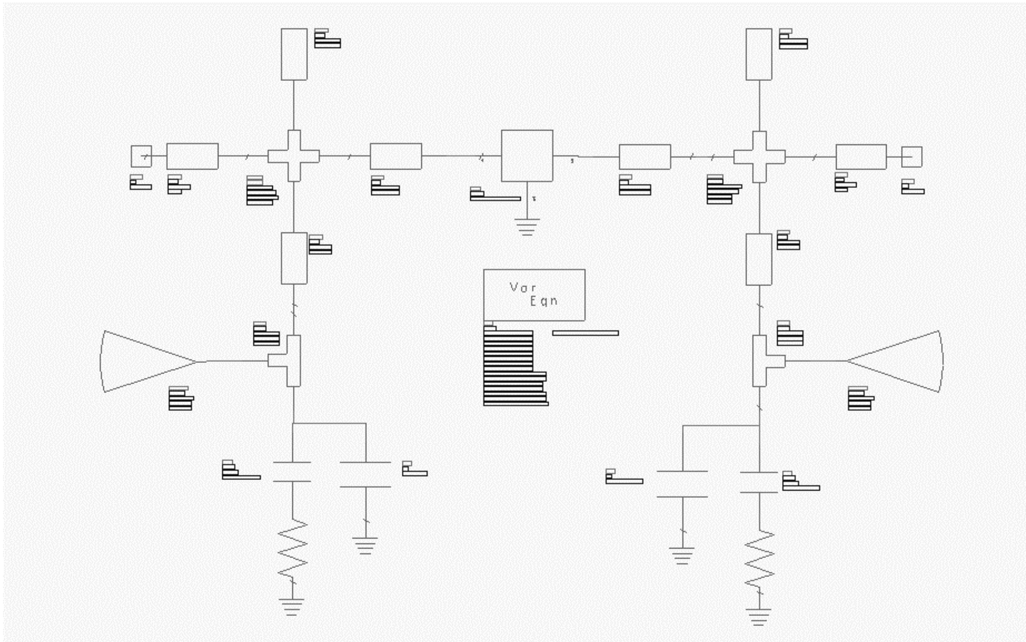

Fig 4.6. Schematics of Single Stage Amplifier

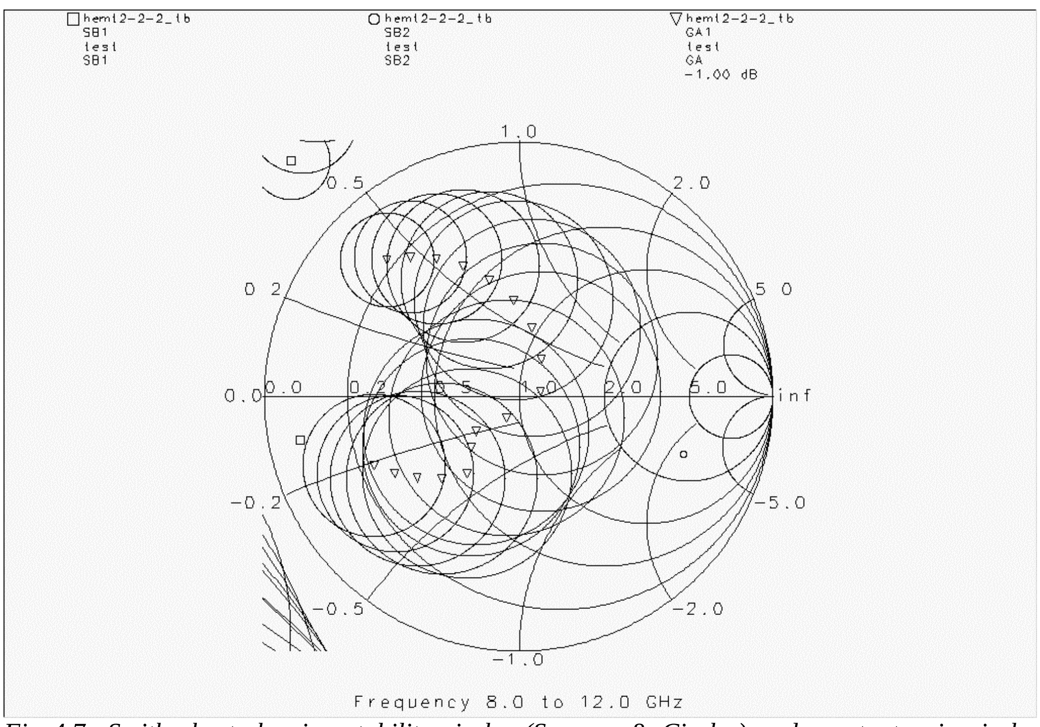

Fig 4.7 Smith chart showing stability circles (Squares & Circles) and constant gain circles (Triangles)

4.3.2 Maximal Transducer Power Gain

The unilateral transducer power gain G_T is the forward power gain in a feedback amplifier having its reverse power gain set to zero (ie. $|S_{12}|=0$) by adjusting a lossless reciprocal feedback network connected around the microwave amplifier [4.1]. This is given by

$$\begin{aligned} G_T &= \frac{1-|\Gamma_S|^2}{|1-\Gamma_{in}\Gamma_S|^2}|S_{21}|^2\frac{1-|\Gamma_L|^2}{|1-S_{22}\Gamma_L|^2} \\ &= \frac{1-|\Gamma_S|^2}{|1-S_{11}\Gamma_S|^2}|S_{21}|^2\frac{1-|\Gamma_L|^2}{|1-\Gamma_{out}\Gamma_L|^2} \\ &= G_S G_O G_L \end{aligned} \qquad (4.10)$$

Hence the transducer's gain is the combination of gains obtain from input matching circuit, active device, and that of output matching circuit. It can be seen that for a particular HEMT, G_o is fixed, therefore the transducer's gain is completely relied upon the changes in the matching circuits.

The maximum transducer power gain G_{Tmax} that can be realised is the forward power gain when the input and output of the amplifier are simultaneously conjugate matched. By this it is meant that the source and load reflection coefficients Γ_s, Γ_L is equal to the conjugate of input and output reflection coefficients Γ_{in}, Γ_{out} respectively (ie. $\Gamma_s=\Gamma_{in}^*$, $\Gamma_L=\Gamma_{out}^*$). The optimal reflection coefficients Γ_{SM}, Γ_{LM} for source and load can be found by

$$\Gamma_{SM} = \frac{B_1 \pm \sqrt{B_1^2 - 4|C_1|^2}}{2C_1} \qquad (4.11) \qquad\qquad \Gamma_{LM} = \frac{B_2 \pm \sqrt{B_2^2 - 4|C_1|^2}}{2C_2} \qquad (4.12)$$

$$B_1 = 1 + |S_{11}|^2 - |S_{22}|^2 - |\Delta|^2 \qquad (4.13) \qquad\qquad B_2 = 1 + |S_{22}|^2 - |S_{11}|^2 - |\Delta|^2 \qquad (4.14)$$

The power gain G_s or G_L then forms constant gain circles on the Smith Chart according to the match, where any solution of Γ_s and Γ_L along a specific gain circle would result in power gain of that amount of specific decibels. The constant gain circles for the single stage amplifier is shown in figure 4.7, denoted by triangles.

4.3.3 Input and Output Matching Circuits

To achieve conjugate matching ($\Gamma_s=\Gamma_{in}^*$, $\Gamma_L=\Gamma_{out}^*$), Γ_{in} and Γ_{out} calculated from S-parameters in manufacturer's data sheets are plotted on the Smith Chart. Then 50Ω lines of appropriate lengths can be used in both series and shunt configuration to transform the mismatch of the amplifier to characteristic impedance of 50Ω. In this design, single stub tuning was utilised to save circuitry space as well as providing a more simplistic approach.

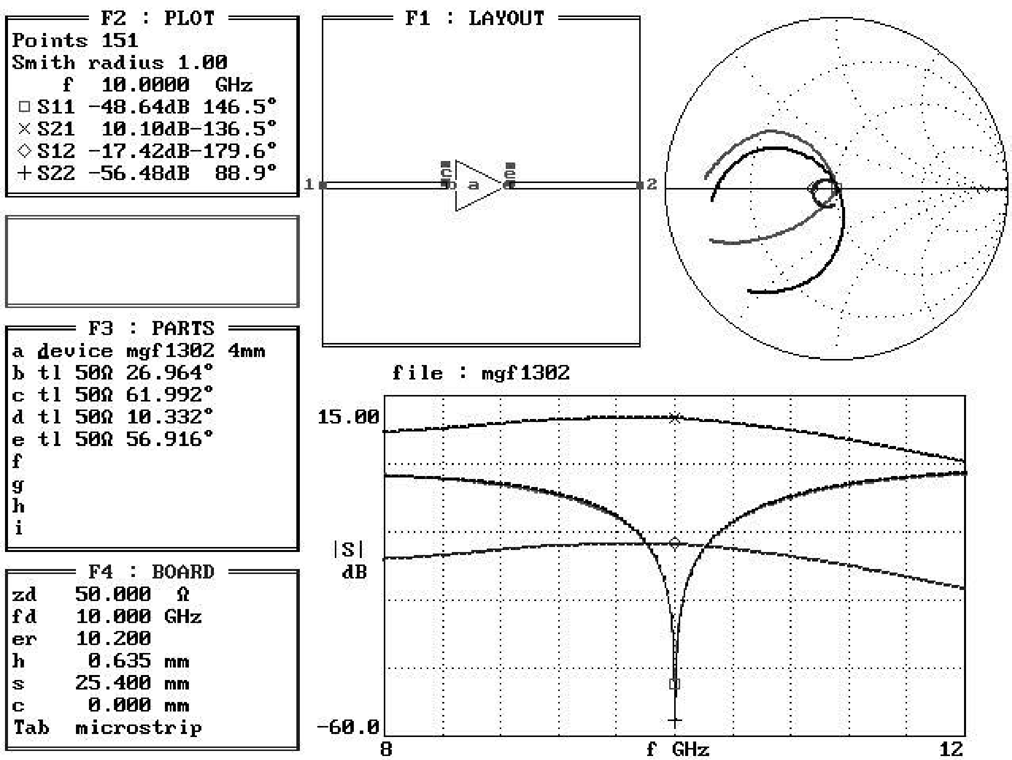

Fig 4.8. Active stage with matching circuits under simulation in PUFF

The theoretically devised matching circuits were then simulated under *PUFF* to ensure feasibility and adjustments were made where appropriate to achieve perfect impedance matching. The simulation results are shown in figure 4.8.

4.3.4 DC Bias

The design of dc-biasing circuits for microwave amplifiers is as important as the design of the matching networks for the amplifiers because the amplifiers' high gain, high power, high efficiency, and low noise also depend on the dc-biasing circuits. The purpose of dc-biasing circuit design is to provide a proper quiescent point and hold that point constant over temperature and device-parameter variations.

For the design of the biasing circuitry, it is important to recognise the biasing conditions for which the adopted design S-parameters were measured. Hence, for the single active stage, the recommended biasing conditions (V_{ds}=3V, I_{ds}=10mA) were implemented according to the manufacturer's data sheets given in Appendix A. This is the same biasing conditions used to determine the S-parameters apply in other sections of this design.

The bias circuitry is shown as the bottom part of figure 4.6. It is connected to both the gate and drain, while the source remains ground. This source grounding technique is employed for the purpose of reducing instability problems associated with excess inductance between source and ground. Each biasing construction consists of a quarter-wavelength open circuit radial stub has the effect of making the DC-RF T-junction intersection realising effectively a short circuit. This RF choke serves the purpose of isolating RF signals from DC to prevent signals being grounded through dc-biasing line. The remaining RC network is design to provide low frequency stability for the network, it consists of a parallel capacitor (10nF) configuration with one branch in series with resistor of value 47Ω, these values were chosen deliberately so the amplifier realises an open circuit at near dc frequencies.

The complete amplifier design was then drawn into the schematic of *HP-EEsof Touchstone (Series IV)*, where the CAD software performed optimization on various key parameters of the circuit until desired S-parameter responses were achieved and physical layout of the circuit generated. Shown in figure 4.9 is the simulation result of the amplifier's 2-port S-parameters.

Observation of figure 4.9 reinforces the expectation of a very good matching circuit achieved through *PUFF* and *Touchstone*, with input reflection coefficient (S_{11}) providing –10dB impedance bandwidth of 11.3% and 23.7dB input return loss at the 10GHz design frequency. The gain (S_{21}) is at 10.2dB with –3dB bandwidth of 30.4%. Isolation (S_{12}) is reasonably low at –19.3dB while output reflection coefficient (S_{22}) achieved an output return loss of –18.8dB and bandwidth of 16.3%. These results suggest good gain characteristics obtainable from the HEMT amplifier at the design resonant frequency.

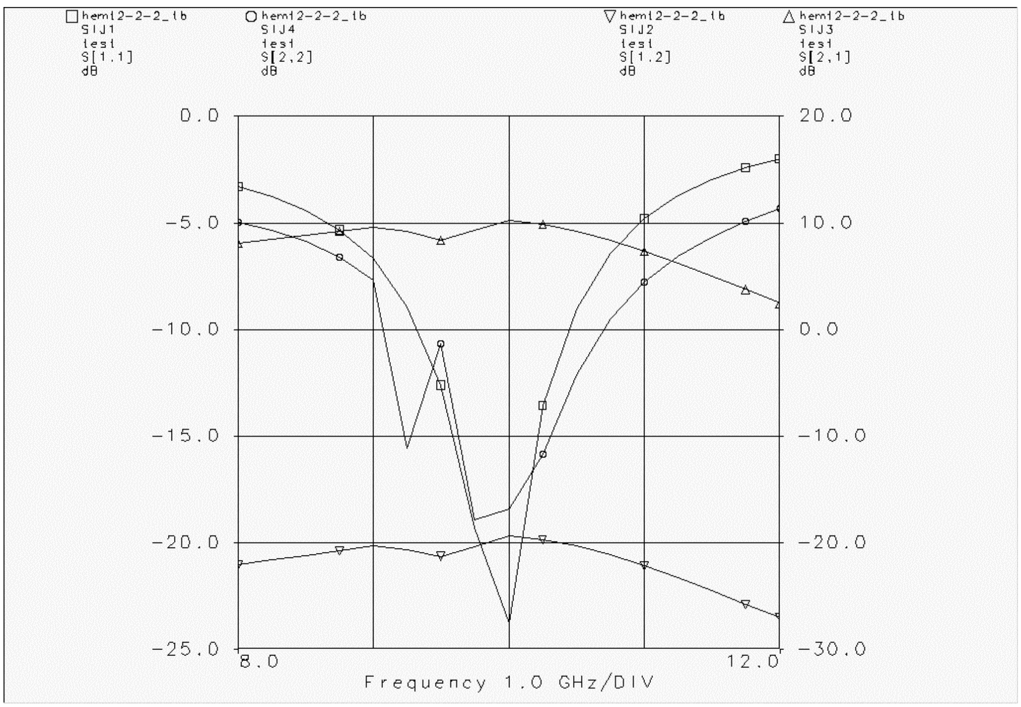

Fig 4.9. Touchstone Single Stage Amplifier S-parameter simulation

4.4 QUASI-OPTICAL UNIT CELL & ARRAY DESIGN

Presented in figure 4.10, 4.11 are the quasi-optical unit cell and 2x2 array amplifiers in their actual sizes, respectively. The unit cell measures 38.1mmx25.4mm(WxH), while the 2x2 array occupies only 88.9mmx61mm(WxH) of space. The unit cell is the combination of two ACMA patches (transmitter and receiver in opposite polarization) with the single active stage forming a transceiver structure. Direct connection of feed lines was made possible by the fact that all microstrip line widths were design upon the characteristic impedance of 50Ω, hence, there was no need for extra matching circuitry. This simple and straightforward integration process not only provide significant reduction in space, it also saves time and cost incurred in the designing process.

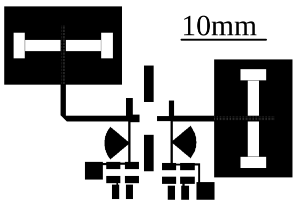

Fig 4.10. Actual size representation of quasi-optical unit cell amplifier

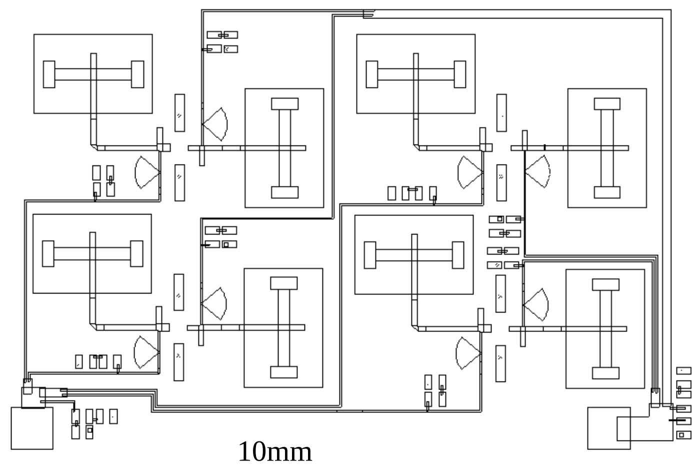

Fig 4.11. Actual size representation of quasi-optical 2x2 4-element array amplifier

The 2x2 4-element array layout was created using *Layout* function in *Touchstone*. It serves the purpose of increasing directive gain to produce narrower beamwidth, as well as to provide improved power handling capabilities to overcome the low-power characteristics common to microstrip antennas. By introducing feeding and combining in free space, this quasi-optic method eliminates much of the feed losses in conventional circuit and waveguide combiners. However, due to the relatively large size of the unit cell, element spacing requirement of less than one wavelength ($d<\lambda$) could not have been achieved. Therefore an increase in grating lobes will be definite; the only real solution that may be applied to rectify the problem is by arraying into larger structures to reduce spacing distance.

In the design process, there was a need to transform impedances of lines to ensure correct and equal current distribution to each of the four transistor amplifiers. Although conventional resistor current divider network could have achieve this, it would have led to a bulkier and heavier design. Therefore, a unique impedance-dividing network was utilised; the concept of is illustrated graphically in figure 4.12.

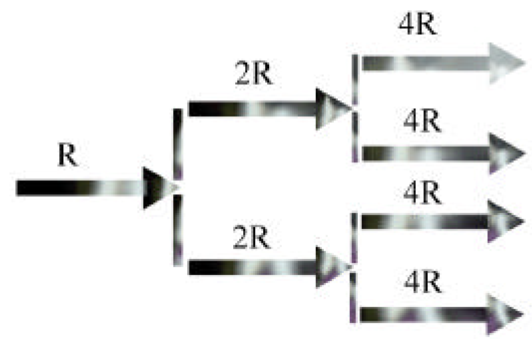

Fig 4.12. Impedance dividing network

With this method, lines of different widths were used to represent the impedance required. As a result, to distribute equal current of 10mA to each amplifier, a total of 40mA has to be fed from the source.

REFERENCES

[4.1] Liao S.Y., “Microwave circuit analysis and amplifier design”, *New Jersey: Prentice-Hall, 1987.*

[4.2] Cheng D. K., “Field and Wave Electromagnetics”, *Sydney: Addison-Wesley, 1989.*

[4.3] Cheng K., “Microwave Solid-State Circuits and Applications”, *Brisbane: John Wiley & Sons, Inc, 1994.*

[4.4] Medley M. W., “Microwave and RF circuits: Analysis, Synthesis and Design”, *London: Artech House, 1992.*

CHAPTER 5

RESULTS AND DISCUSSION

This chapter is concerned with presenting experimental results, discussing them by comparing with simulations and to justify the discrepancies observed by relating to the theory and concepts the design originated from. The results will be discussed in the following order:

1) ACMA patch S_{11} input return loss measurement.
2) Single active stage amplifier 2-port S-parameter measurements.
3) 2 x 2 array quasi-optical amplifier gain measurements.
4) 2 x 2 array quasi-optical amplifier far-field radiation measurement.

The measurement techniques adopted were very similar to that described in C. H. Wong's thesis [1.6], the reason for this is so that a close comparison can be obtained between these two projects to show the improvements gained from using ACMA as opposed to edge feeding single layer antenna. However, due to equipment shortages, the task of performing some experiments was impossible, despite this, the majority of experiments were undertaken and promising results were obtained.

The setup apparatus used in measuring each of the prototypes are as shown in figure 5.1-5.4. In all experiments, results were generated on the display of Hewlett Packard's 83651A 8360 series synthesized sweeper. For the testing of antenna patch input return loss and single active stage amplifier 2-port S-parameters, Hewlett Packard's model 8530A microwave receiver vector network analyser (VNA) and model 8517A s-parameter analyser were employed as shown in figure 5.1&5.2. With the measurement of the quasi-optical amplifier gain, beside the inclusion of two horn antennas, an added power source (either battery pack or power supply) is required to provide dc biasing and power to transistor. The use of far field absorbers as shown in figure 5.3 is also necessary to eliminate unwanted energy reflection from surrounding environment. While the above measurement requires relatively no insulation to

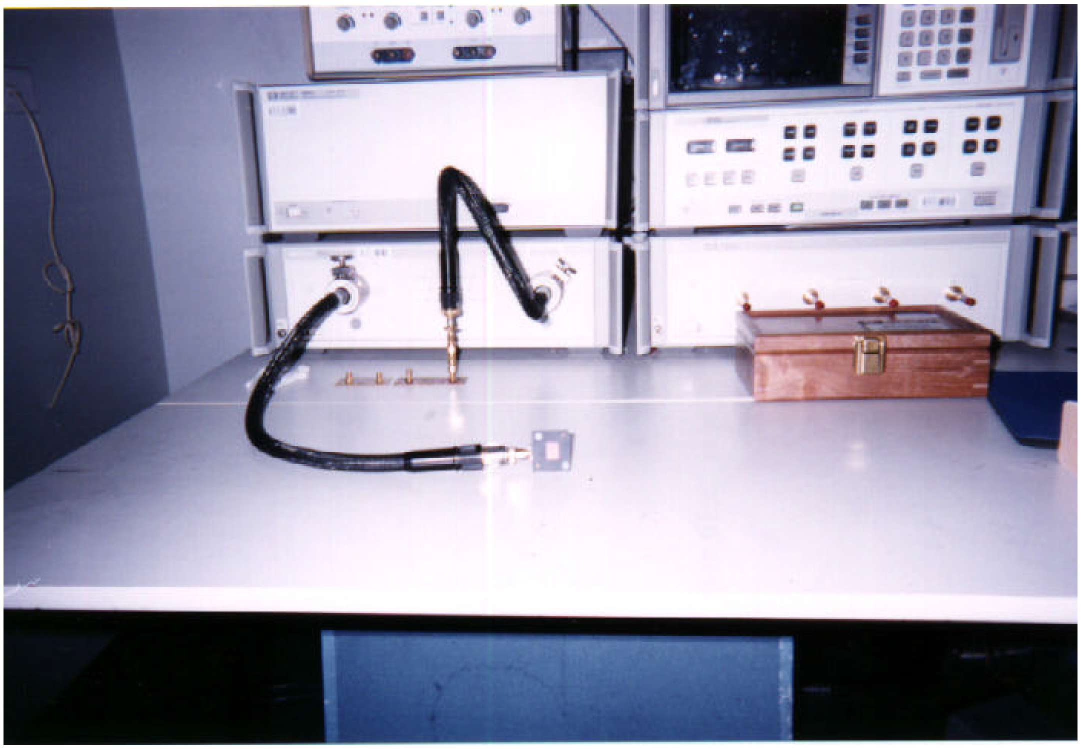

Fig 5.1. ACMA patch under test with HP VNA

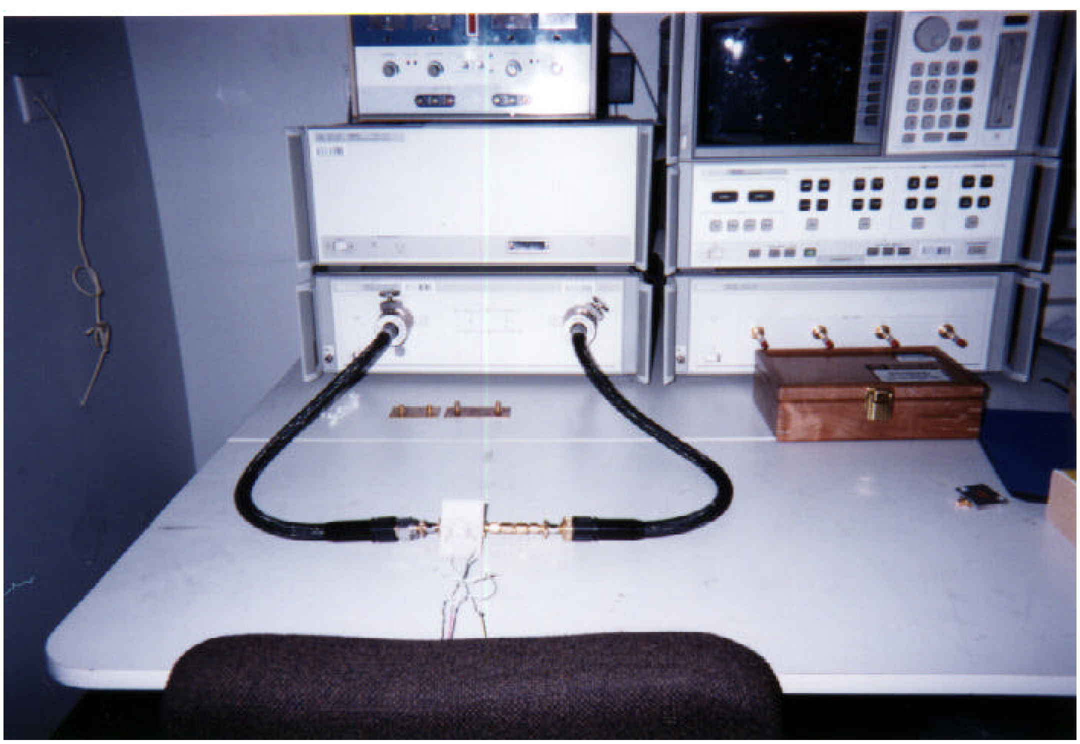

Fig 5.2. Single Stage Active amplifier under test with VNA

Fig 5.3.Experimental setup for quasi-optical amplifier gain measurement

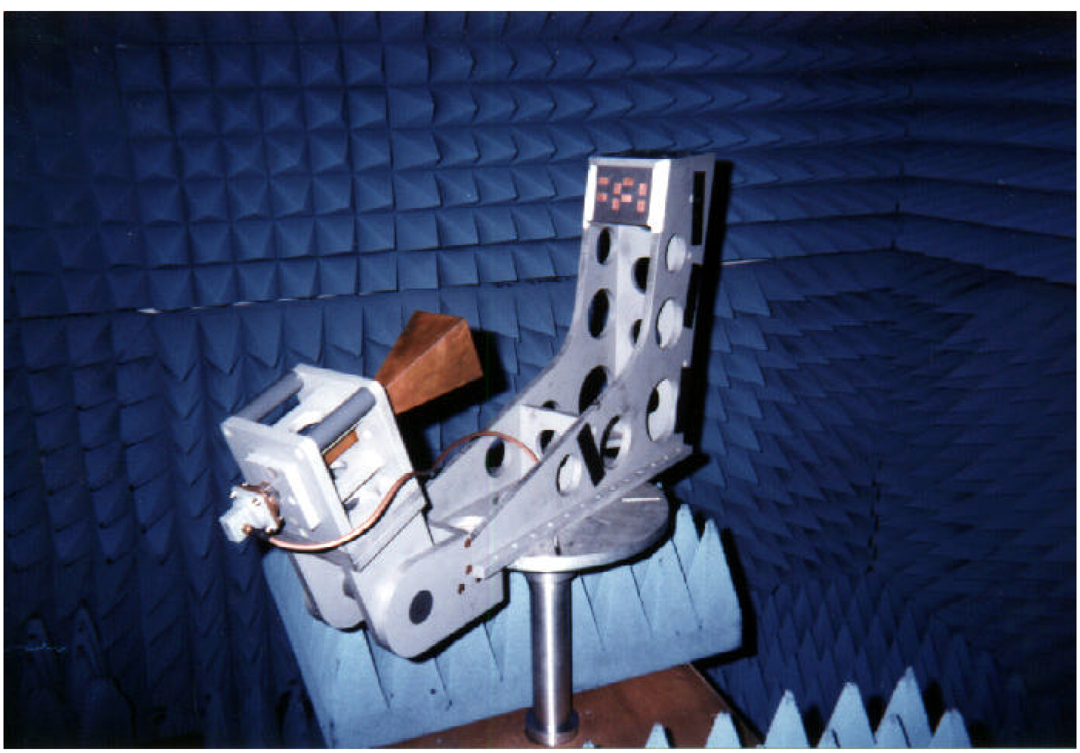

Fig 5.4. Experimental setup in anechoic chamber for radiation pattern measurement

surrounding environment, when measuring the far field radiation pattern, the additional use of anechoic chamber is essential to produce the best results, the test setup for this is illustrated in figure 5.4.

5.1 ACMA PATCH S_{11} MEASUREMENT

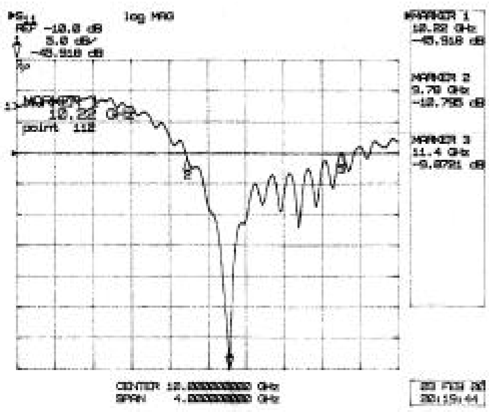

Fig 5.5a. Patch S_{11} measurement

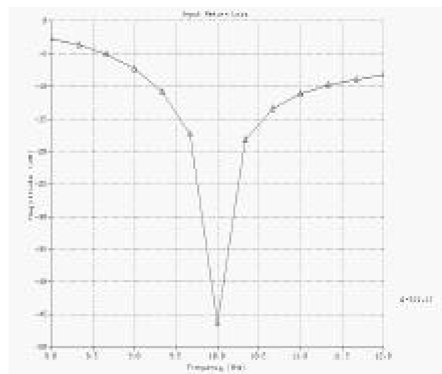

Fig 5.5b. Patch S_{11} simulation

For the measurement of S-parameters using the Hewlett Packard setup, it is necessary to calibrate the port(s) of interest, irrespective of the use of either port 1 or 2 or both. This is to ensure the equipment is tune to produce optimal results within the operating range of frequency. The actual experimental setup is shown in figure 5.1.

Figure 5.5 a & b shows a comparison between the measured S_{11} characteristics with that obtained through *Ensemble* simulation. The measured result gave a bandwidth of almost 17% with input return loss of –45.918dB at a resonant frequency of 10.22GHz, this is very similar to the simulated figures of 21.5% and –47dB return loss. Such results can be considered very good with the only noticeable differences being 4.5% BW reduction and frequency shift of 0.22GHz. The most likely reasons to account for such discrepancies are probably related to manufacturing errors and misalignment of the dielectric substrate layers. With the alignment of three substrate layers (antenna, foam, and feed) totally relied upon alignment holes, imperfections are bounded to occur due to human inaccuracies in both drilling and aligning the holes. Other factors that would have added to the negative effect of this are:

- Air gaps due to substrate imperfections.
- Poor soldering connections causing mismatch.
- Probe connector losses.

Nevertheless, the promising experimental result reinforces the theory that aperture coupling has strong ability to greatly enhance bandwidth.

5.2 SINGLE STAGE 2-PORT S-PARAMETER MEASUREMENTS

For the single active stage measurement, the VNA required a full 2-port calibration. The setup for measurement of the active stage is shown in figure 5.2. The experimental plot for various 2-port parameters are shown in fig 5.6 a – d.

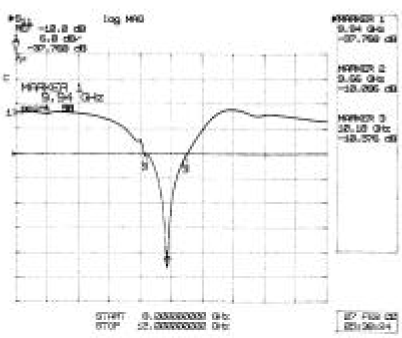

Fig 5.6a. Single stage S_{11} input return loss

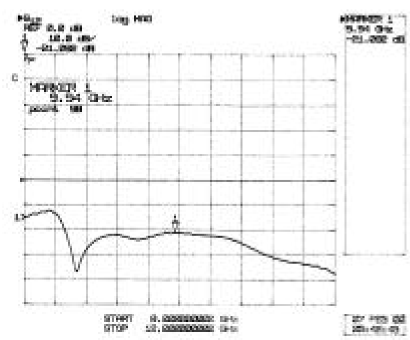

Fig 5.6b. Single stage S_{12} reverse transmission coefficient

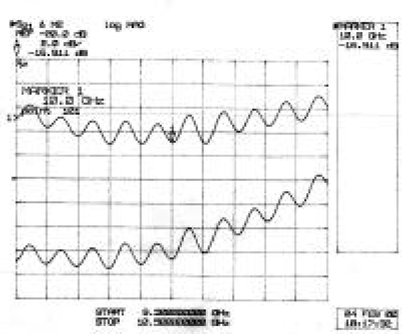

Fig 5.6c. Single stage S_{21} gain (forward transmission coefficient)

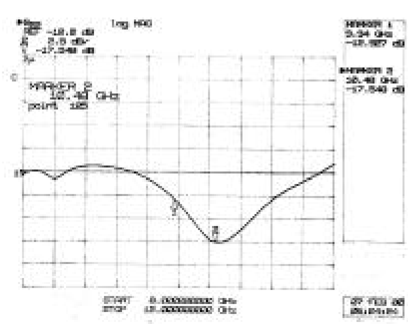

Fig 5.6d. Single stage S_{22} output return loss

The results from the S-parameter plots of figure 5.6, together with those from the simulations of *Touchstone* are summarised in table 5.1.

	S-parameter	Measured Frequency (GHz)	Value at frequency (dB)	% Impedance/ -3dB BW (Gain)
Experimental measurements	S_{11}	9.94	-37.768	5.2
	S_{12}	9.94	-21.092	NA
	S_{21}	10	10	-
	S_{22}	10.48	-17.548	24
Simulation results	S_{11}	10	-23.7	11.3
	S_{12}	10	-19.3	NA
	S_{21}	10	10.2	30.4
	S_{22}	10	-18.8	16.3

Table 5.1. Summary of figures obtained in experiment and simulation

The experimental result for S_{11} showed figures that was a little disappointing, not only was there a decrease in input return loss at a -0.06GHz frequency shift, the impedance bandwidth almost halved that of expected. The output reflection coefficient suffered similar degrade in performance leading to a relatively large frequency shift of 0.48GHz, but with a surprising increase in impedance bandwidth of 7.7%. While the isolation and gain remained in relatively close agreement with the simulations demonstrating the desired characteristics, the author was unable to obtain an analysis of the absolute isolated gain to compare with that of simulated. This was due to an unfortunate incidence where electrostatic charge damaged the HEMT amplifier a short time after obtaining the first set of results. Nonetheless, the relative gain graph demonstrates the practicality of achieving the theoretical 10dB gain achievable with the active stage. The most probable reasons that contributed to the poor measured results are:

- Poor soldering connections causing mismatch.
- Dielectric substrate imperfections.
- Overlapping between transistor legs (gate and drain) with the relatively tiny matching circuits. Therefore, although perfect matching circuits were design, the microscopic nature of microstrip circuitry makes establishing perfect connections very difficult.

- Variations of S-parameter values between manufacturer's data sheets and that of the actual device used, where the difference in test environment may also account for some disagreement.
- Basically due to unavoidable human error within the fabrication process.

5.3 2 X 2 ARRAY QUASI-OPTICAL AMPLIFIER GAIN

The experimental setup for a quasi-optical amplifier is somewhat different to that used for the active stage in figure 5.2 because the feeding and combining activity takes place in free space, thus eliminating the use of conventional measurement approach whereby probes are connected to input and output via physical connectors. Therefore, a technique similar to that used in radar systems is employed, where a signal is transmitted towards the antenna amplifier, and measurements are obtained through the amplified signal reflected to a receiver. The experimental test setup is presented in figure 5.3. It should be noted that transmitter and receiver horns utilises opposite polarizations (vertical and horizontal) to match the orthogonal polarization used in antenna patches on the quasi-optical amplifier, the purpose of this is to reduce the level of cross polarization.

As describe in earlier sections, quasi-optical technique when employed in an array structure, it provides two key advantages:

1) 100% power combining efficiency significant increase gain from individual solid state devices. Therefore, gain is increased by the factor equal to number of unit cells used.
2) Due to intrinsic redundancy of individual elements in the array, graceful degradation is observed rather than catastrophic failure when performance of the devices deteriorates.

In order to demonstrate the effect of quasi-optics in an array, the 2x2 quasi-optical amplifier circuit was first switched off to provide a gain plot for zero element. Then a similar plot was obtained to show the contribution of two elements by switching on the array with half of the four elements blocked off by absorbers. The final step was to measure the gain with all four elements exposed. The gain plot obtain is given in figure 5.7 and the results from these experiments are summarised in table 5.2.

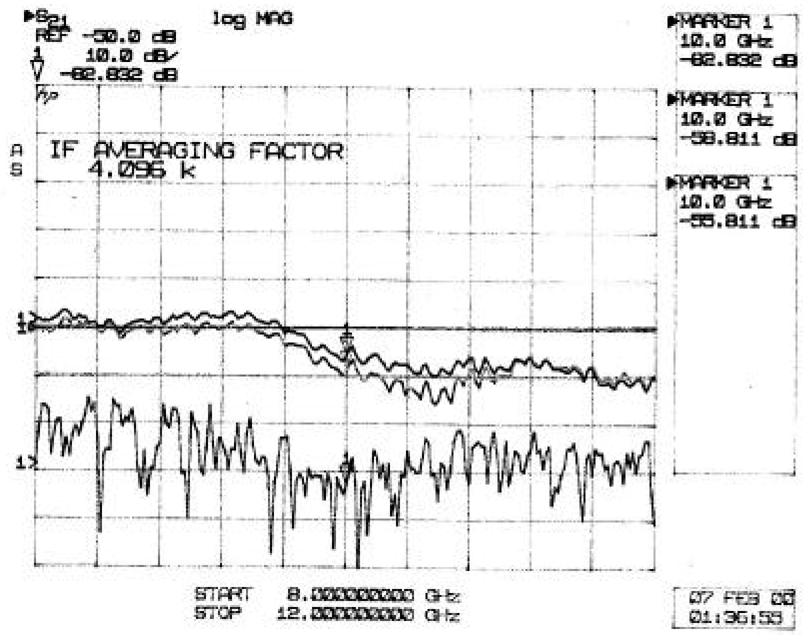

Fig 5.7. Gain plot for 2x2 array amplifier with 0, 2, 4 elements switched on

Elements on	***0***	***2***	***4***
Measured Gain relative to zero element (dB) at 10GHz	0	24.021	27.021

Table 5.2. Experimental measurements for 2x2 array quasi-optical amplifier with 0, 2, 4 elements exposed.

The concept of quasi-optical amplifier is demonstrated with 2 element gain being exactly 3dB (half power) below the 4element configuration, therefore 100% power combining efficiency is verified. At the same time, the theory of intrinsic redundancy within array element is also experimentally proven, by simply covering up half of the array, there was no sign of any effect upon the exposed portions, and operation was as usual with expected gain being halved from the full array. Hence, in practise, quasi-optcal technique is highly feasible, and certainly lives up to its expectations in providing its theoretical advantages of both 100% combining efficiency and graceful degradation rather than catastrophic failure.

It was shown in section 5.2 that the measured gain from the single active stage transistor (without the transmitting and receiving patch antennas) is 10dB. Thus the gain from each patch antenna can be easily calculated by:

$$\text{Total Measured gain } (G_{MEAS}) = \text{no. of unit cells} \times G_{AMP} \times G_{Tx} \times G_{Rx} \qquad (5.1)$$

Since the transmitting and receiving patch are identical, therefore G_{Tx} and G_{Rx} are the of equal value and thus modifies equation 5.1 to:

$$\text{Total Measured gain } (G_{MEAS}) = \text{no. of unit cells} \times G_{AMP} \times G_{PATCH}^{2} \qquad (5.2)$$

$$\text{In dB} \rightarrow \quad 27.021\text{dB} = 10\log 4 + 10\text{dB} + 2[G_{PATCH}]_{dB} \quad [\text{dB}]$$

$$[G_{PATCH}]_{dB} = 5.5\text{dB}$$

To explain why the patch gain does not closely match with the 8dB shown in the simulation of figure 4.2, there are numerous possible factors:

- The most influential being the increased number of transistors leading to additional soldering, and hence the possibility of mismatches was severely elevated. As shown in the active stage, this mismatching can seriously degrade the performance of the output.
- The 8dB gain obtain in the simulation was never actually tested experimentally due to equipment incapabilities. Thus, one cannot be certain that the experiment test patch can actually produce that level of gain from the simulation.
- The overall gain could have been reduced due to the inefficiency in the test environment setup, for example, the misalignment between the transmitting and receiving horns with the planar antenna amplifier can result in rather significant gain reduction.
- The mutual coupling between the horns is difficult to avoid or eliminated when being so close in distance with each other, this could have again led to discrepancies in the measured results. Mutual coupling of patches could have added effects to this also.

Nonetheless, the important aim of this experiment was to verify the concept of quasi-optical combining, which was very successfully demonstrated by achieving double power in the 4-element array with respect to 2-element array.

However, there are concerns for erroneous combining efficiencies considerably over 100% when such high combining efficiencies cause impedance variations leading to undesired reflections in both source and load of the transistor amplifier [5.2].

5.4 2 X 2 ARRAY FAR FIELD RADIATION PATTERN

The radiation pattern provides useful radiation characteristics of the antenna in terms of its directivity, which is extremely important for suitability in WLAN applications. The mechanical setup for positioning the array amplifier and receiving horn is illustrated in figure 5.4. In this configuration, the horn rotates with the amplifier in full 360° to obtain the radiation pattern. Another stationary horn (not shown in picture) acting as transmitter is positioned several metres away to provide signal to the amplifier. The use of far field anechoic chamber with electromagnetic absorbers is essential to eliminate the unwanted stray radiations.

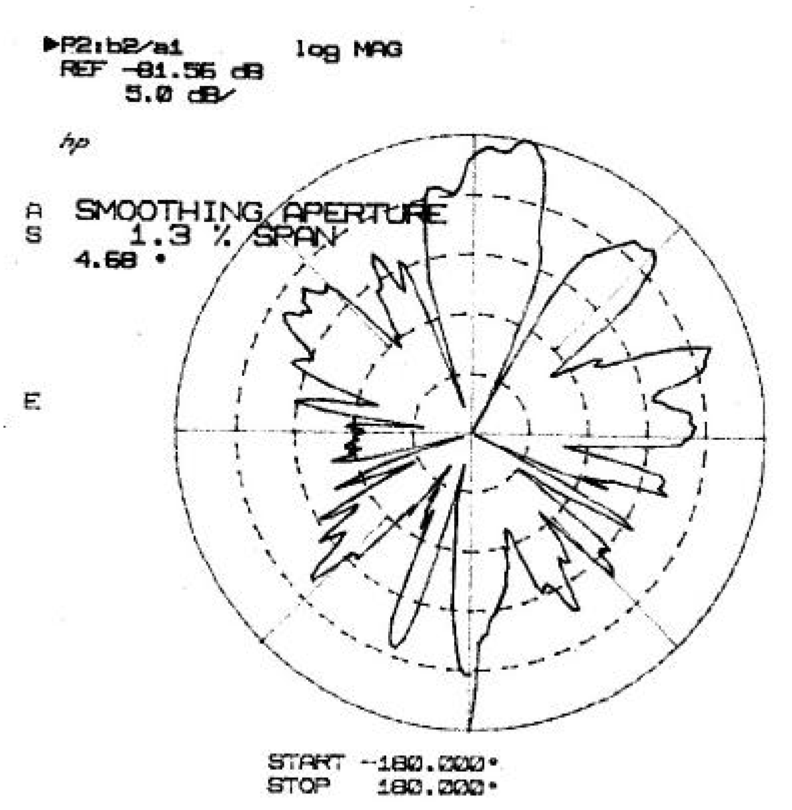

Fig 5.8. Radiation pattern of 2x2 array quasi-optical amplifier

The measured radiation pattern is shown in figure 5.8. A –3dB half power beam width (HPBW) of 16° is observed with two major grating lobes of –3dB level offset at 31° and 58°. From the theory section, it was expected that significant side lobe levels would occur due to the unavoidable element spacing of greater than one wavelength apart, and because only four elements are arrayed, it was very difficult to completely eliminate side lobe occurrence. However, this can be overcome by construction of larger arrays by utilising a 4-element sub-array as the unit cell, which provides increase space and flexibility to implement closer spacing. A larger array will not only considerably reduce side lobe levels to an acceptable level, it will also result in a narrower main beam with improved directive gain. This is very desirable in WLAN use as it permits closer spacing between remote terminals where the reduced sidelobe amplitudes will minimise crosstalk within nearby stations. The experimental result suggests that the current design has the ability to accommodate remote terminals within a range of 16° spread, however, this will greatly improve as the array size increases to provide a more directive beam. In effect, the network's capacity will increase as it can accommodate more users per microcell.

Another reason for the high level of side lobes could again be due to experimental flaws. For instance, in can be seen from the setup of figure 5.4 that the receiving antenna's vertical position is in very close proximity to the signal path from transmitter to amplifier. This could cause quite a significant level of coupling between the transmitter and receiver when the experiment is being conducted, and thus resulting in higher levels of side lobes. To minimise this, one could have placed the receiver at a lower level than that shown in figure 5.4, but this is not always possible due to equipment constraint and will result in a signal decrease at the receiver due to angle offset. Another solution would be to place extra absorbers surrounding the receiver horn to minimise the level of coupling between it and the transmitter. The mutual coupling between patches on the array may also account for some of the effects shown in the radiation pattern, the only solution to this is by careful arrangement of antenna patches on the array during the design stage. Beside this however, there is very little that one can do to completely rectify this problem.

Nevertheless, the 4-element array showed very promising results for potential use in WLAN applications, although current array size is unsuitable due to high level of side lobes, a larger array will definitely provide a real compelling solution.

REFERENCES

[1.6] Wong C. H., “A Steerable Planar Antenna System for Wireless LAN”, *University of Queensland, 1996.* **(Specifically re-referenced to conduct replicated measurement for comparison)**

[5.2] Zurcher J. F., “Broadband patch antennas”, *Norwood: Artech House, 1995*

CHAPTER 6

CONCLUSIONS AND FUTURE DEVELOPMENTS

6.1 CONCLUSIONS

A 10GHz quasi-optical planar array antenna, designed for conformal use on a millimetre wave wireless LAN reflection-mode relay station was proposed. The motivation for this came from the ever-increasing demand of mobile terminals within a local area network. Therefore the design of this antenna system is intended to significantly cut down expensive cabling and labour costs commonly associated with WLANs.

The trend towards sub-millimetre and millimetre wave frequency operation is to provide considerable increase in bandwidth from these unregulated spectrums. Along with the bandwidth increment comes the advantages of higher data throughput rate and robust communication link, which are essential for WLAN applications. The use of high millimetre wave frequency is also advantageous for smaller component sizes and better antenna arraying characteristics favourable for antenna use in WLAN relay stations.

Nonetheless, the major limitation with the use of millimetre wave exists for low power handling capabilities of solid state devices. Therefore, a technique known as power combining is utilised in an attempt to boost the output power level obtainable from many of these devices. Furthermore, due to high conductor feed losses associated with conventional combining method, a new approach must be devised.

This has led to the use of quasi-optical power combining technique in this thesis. With this new method, power is fed and combined in free space with 100% efficiency. It also offers the advantages of providing higher directivity and narrow beamwidth ideal for angle diversity used for electronic beam steering in a WLAN environment. It also provides the desirable characteristic of graceful component degradation as opposed to catastrophic failure, which is an excellent feature for WLAN use, as sudden total collapse in a network environment would lead to enormous loss in any business.

In order to produce a conformal product, conventional antenna structure cannot be employed, because at such high frequency there are many constraints with manufacturing tiny structures of such shapes. Even if fabrication process permits the assembly to be formed, it would not be flexible nor would it be flat enough to conform on near flat surfaces. Hence the use of microstrip antenna is required.

Although microstrip antenna has many of the ideal characteristics for WLAN such as low profile/size/weight and low cost, it suffers from narrow bandwidth and high losses. Thus, in the design of the antenna system, effective microstrip structure and innovative amplifying approach is essential.

The antenna design used in this thesis utilised aperture coupling architecture due to its renowned reputation of bandwidth enhancement. Also employed in this design was the use of low noise HEMT (High Electron Mobility Transistor) to provide the required gain. The combination of these forms a unit cell, which is used to implement larger arrays that takes advantage of the use of quasi-optical power combining to provide efficient output in order to overcome the low power of individual unit cells.

The design process for determining various dimensional parameters on the antenna patch and amplifier matching circuits was heavily computer involved. The software used includes *Ensemble* by Microwave Boulder technologies for designing of patch, *PUFF* was used for designing the preliminary matching circuits due to its simplicity and simulation speed, finally both patch and amplifier are integrated into a single structure with *HP-Eesof Touchstone* by Hewlett Packard.

For the measurement of the antenna patch, a 17% impedance bandwidth was achieved with input return loss of –45.918dB at resonant frequency of 10.22GHz. These results match very closely to that obtained from *Ensemble* simulation of 21.5% and –47dB at 10GHz. Thus, the theory of improved bandwidth through aperture coupling does live up to its expectation when compare to previous edge fed design of only 4% achievable impedance bandwidth.

The resultant 4-element array amplifier measures only 88.9mmx61mm(WxH) while the unit cell structure occupies 38.1mmx25.4mm(WxH). Its measured gain at 10GHz was 27.021dB with calculated patch gain of 5.5dB, and its radiation pattern provided a –3dB HPBW of 16° with major grating lobes of –3dB down offset at 31° and 58°.

The practicality of quai-optical power combining technique was demonstrated by having a portion of the array blocked off and leaving only 2-element exposed for measurement. The gain achieved from this was 24.021dB, exactly 3dB down from that of 4-element array, suggesting only half of the power, and therefore provided experimental proof of the quasi-optical technique's 100% power combining efficiency and graceful degradation characteristics.

Although the current 4-element design is still quite impractical for use in a practical WLAN environment due to the large level of side lobes, the concepts used and the results obtained suggests very high potential for such a design. If the drawbacks can somehow be eliminated, the proposed design would provide an extremely feasible and compelling solution to the WLAN market.

6.2 FUTURE DEVELOPMENTS

The most obvious and required future development to continue this project would be the formation of a larger 16x16 array. In accomplishing this, the side lobe levels would be greatly reduced, enabling the design to achieve good angular diversity for beam steering in WLAN applications. In doing so, the gain would also increase proportionally; the increase in directivity would also lead to narrow beams so accommodating more users expanding the network's capacity.

It has been illustrated in this thesis that a multi-layer configuration can considerably increase bandwidth over single layer structures. Hence one can take this approach further by adopting a stack construction. It has been shown in many other experiments that a stack configuration can improve bandwidth of aperture coupled microstrip antennas to even 50%, primarily due to the double tuning effect introduced [6.1,6.2,6.3,6.4]. With the increase in bandwidth, a more robust and higher throughput channel can be achieved.

Instead of dual polarization, one might like to employ the use of circular polarization as it provides better penetrating property [6.5]. Thus the negative effects of multipath propagation can be significantly reduced, which again helps to provide better data throughput favour in WLAN.

Furthermore, instead of having separate transmitting and receiving patch antennas to achieving orthogonal polarization, the use of a dual polarized can be employed to save more precious substrate space. This would provide a solution for the spacing problem encountered in this thesis as the spacing distance between adjacent antenna patches can be significantly decreased. However, this configuration suffers from the problem of limited isolation between transmitting and receiving feed [3.6].

Finally, the current status of the 4-element array cannot provide steering control by itself due to the lack of microprocessor controller. Although not in the field of microwave technology, it needs to be addressed, as the antenna cannot operate in any environment without it. Therefore, the development of a protocol for steering control is essential for this antenna system. Moreover, an efficient multiple access method must also be devised to control the large amount of user traffic [1.6].

REFERENCES

[6.1] Croq F., Papiernik A., “Stacked slot-coupled printed antenna”, IEEE Microwave and Guided Wave Letters, vol. 1, pp.288-290, October 1991.

[6.2] Croq F., Pozar D. M., “Millimetre wave design of wide-band aperture coupled stacked microstip antennas”, IEEE Trans. Antennas and Propagation, vol. 39, pp. 1770-1776, December 1991.

[6.3] Targonski S. D., Waterhous R. B., “An aperture coupled stacked patch antenna with 50% bandwidth”, IEEE International Symposium on Antennas and Propagation, Baltimore, MD. 1996.

[6.4] Tsao C. H., Hwang, Y. M., “Aperture coupled Patch Antennas with Wide bandwidth and Dual-polarization capabilities”, Electronic Letters, Vol 21, No. 2, pp. 49-50, Jan 1985.

[6.5] Targonski S., Pozar D. M., “Design of wideband circularly polarized aperture coupled microstrip antennas”, IEEE Trans. Antennas and Propagation, vol. 41, pp.214-220, February 1993.

APPENDIX A

MGF1302 HEMT DATA SHEETS

ATTENTION JOHNSON
RGDS.

MITSUBISHI SEMICONDUCTOR (GaAs FET)

MGF1302

LOW NOISE GaAs FET

DESCRIPTION

The MGF1302 is a low-noise GaAs FET with an N-channel Schottky gate, which is designed for use in S to X band amplifiers and oscillators. The hermetically sealed metal-ceramic package assures minimum parasitic losses, and has a configuration suitable for microstrip circuits.

FEATURES

- Low noise figure NF_{min} = 1.4 dB (MAX.) @ f = 4 GHz
- High associated gain G_s = 11 dB (MIN.) @f = 4 GHz
- High reliability and stability

APPLICATION

S to X band low noise amplifiers and oscillators

QUALITY GRADE

- GG

RECOMMENDED BIAS CONDITIONS

- V_{DS} = 3V
- I_D = 10mA
- Refer to Bias Procedure

OUTLINE DRAWING

Unit: millimeters (inches)

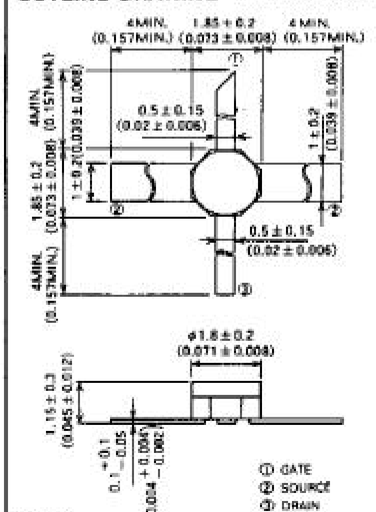

GD-4

ABSOLUTE MAXIMUM RATINGS (Ta = 25°C)

Symbol	Parameter	Ratings	Unit
V_{GDO}	Gate to drain voltage	−6	V
V_{GSO}	Gate to source voltage	−6	V
I_D	Drain current	100	mA
P_T	Total power dissipation *1	360	mW
T_{ch}	Channel temperature	175	°C
T_{stg}	Storage temperature	−55 ~ +175	°C

*1 : Tc = 25°C

ELECTRICAL CHARACTERISTICS (Ta = 25°C)

Symbol	Parameter	Test conditions		Limits Min	Limits Typ	Limits Max	Unit
$V_{(BR)GDO}$	Gate to drain breakdown voltage	I_G = −100μA		−6	—	—	V
$V_{(BR)GSO}$	Gate to source breakdown voltage	I_G = −100μA		−6	—	—	V
I_{GSS}	Gate to source leakage current	V_{GS} = −3V, V_{DS} = 0V		—	—	10	μA
I_{DSS}	Saturated drain current	V_{GS} = 0V, V_{DS} = 3V		30	60	100	mA
$V_{GS(off)}$	Gate to source cut-off voltage	V_{DS} = 3V, I_D = 100μA		−0.3	—	−3.5	V
g_m	Transconductance	V_{DS} = 3V, I_D = 10mA		25	45	—	mS
G_s	Associated gain	V_{DS} = 3V, I_D = 10mA	f = 4 GHz	11	—	—	dB
			f = 12GHz	5	—	—	dB
NF_{min}	Minimum noise figure	V_{DS} = 3V, I_D = 10mA	f = 4 GHz	—	—	1.4	dB
			f = 12GHz	—	—	4.0	dB
$R_{th(ch-a)}$	Thermal resistance *1	ΔV_f method		—	—	416	°C/W

*1: Channel to ambient

MITSUBISHI ELECTRIC

2—6

OCT.01.97 14:25 612 6847208   MEA SEMICONDUCTORS   007 P05

MITSUBISHI SEMICONDUCTOR <GaAs FET>

MGF1302

LOW NOISE GaAs FET

TYPICAL CHARACTERISTICS

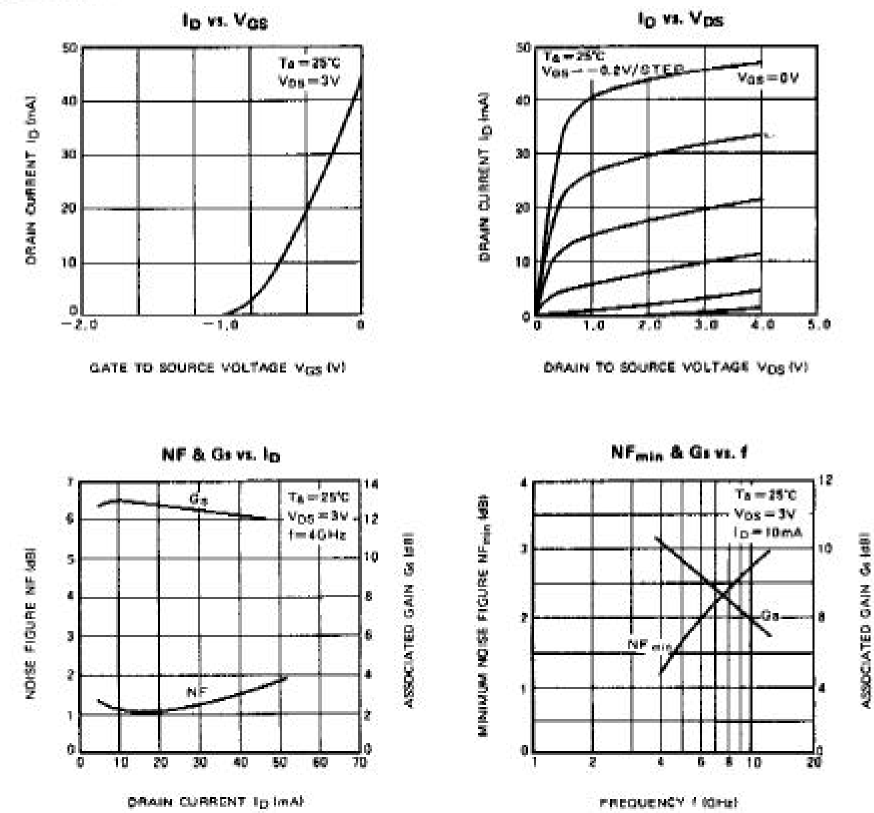

MITSUBISHI ELECTRIC

MITSUBISHI SEMICONDUCTOR <GaAs FET>

MGF1302

LOW NOISE GaAs FET

S_{11}, S_{22} vs. f. S_{21}, S_{12} vs. f.

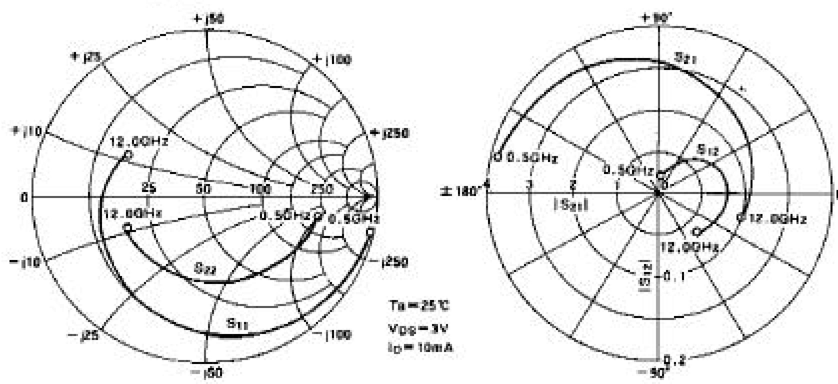

S PARAMETERS (T_a=25℃, V_{DS}=3V, I_D=10mA)

Freq. (GHz)	S_{11} Mag.	S_{11} Ang.	S_{21} Mag.	S_{21} Ang.	S_{12} Mag.	S_{12} Ang.	S_{22} Mag.	S_{22} Ang.	K	MSG/MAG (dB)
0.5	0.997	−13.3	3.809	167.6	0.019	80.1	0.664	−10.3	0.042	23.0
1.0	0.975	−23.1	3.727	158.4	0.026	73.1	0.650	−17.3	0.180	21.6
1.5	0.952	−32.8	3.644	149.1	0.033	66.0	0.636	−24.2	0.271	20.4
2.0	0.929	−42.5	3.561	139.9	0.040	58.9	0.622	−31.2	0.341	19.5
2.5	0.906	−52.2	3.478	130.7	0.047	51.8	0.608	−38.2	0.398	18.7
3.0	0.884	−62.0	3.396	121.5	0.054	44.8	0.594	−45.2	0.449	18.0
3.5	0.861	−71.7	3.313	112.2	0.061	37.7	0.580	−52.1	0.494	17.3
4.0	0.838	−81.4	3.230	103.0	0.068	30.6	0.566	−59.1	0.537	16.8
4.5	0.811	−90.9	3.124	94.4	0.071	24.5	0.551	−66.2	0.604	16.5
5.0	0.783	−100.3	3.018	85.8	0.074	18.5	0.537	−73.3	0.674	16.1
5.5	0.756	−109.8	2.913	77.2	0.076	12.4	0.522	−80.3	0.746	15.8
6.0	0.729	−119.2	2.807	68.6	0.079	6.3	0.507	−87.4	0.822	15.5
6.5	0.709	−127.0	2.710	61.1	0.078	1.1	0.503	−93.7	0.902	15.4
7.0	0.689	−134.9	2.614	53.5	0.078	−4.1	0.499	−100.1	0.989	15.3
7.5	0.670	−142.7	2.517	46.0	0.077	−9.2	0.494	−106.4	1.085	13.4
8.0	0.650	−150.5	2.421	38.4	0.076	−14.4	0.490	−112.7	1.190	12.4
8.5	0.633	−157.6	2.364	31.5	0.075	−18.1	0.487	−118.2	1.271	11.8
9.0	0.617	−164.7	2.308	24.5	0.074	−21.9	0.485	−123.7	1.357	11.3
9.5	0.600	−171.8	2.251	17.6	0.074	−25.6	0.482	−129.2	1.449	10.8
10.0	0.584	−178.9	2.194	10.6	0.073	−29.3	0.479	−134.7	1.547	10.4
10.5	0.568	173.3	2.149	3.4	0.072	−33.9	0.483	−140.1	1.641	10.1
11.0	0.551	165.5	2.103	−3.9	0.071	−38.4	0.487	−145.5	1.739	9.7
11.5	0.535	157.7	2.058	−11.1	0.069	−43.0	0.491	−150.8	1.844	9.4
12.0	0.519	149.9	2.012	−18.3	0.068	−47.5	0.495	−156.2	1.954	9.1

2—8

MITSUBISHI ELECTRIC

MITSUBISHI SEMICONDUCTOR <GaAs FET>

MGF1302

LOW NOISE GaAs FET

S_{11}, S_{22} vs. f.

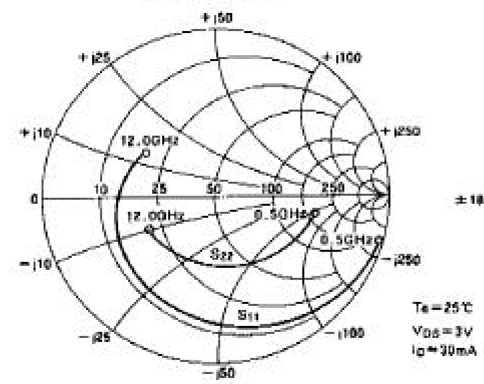

S_{21}, S_{12} vs. f.

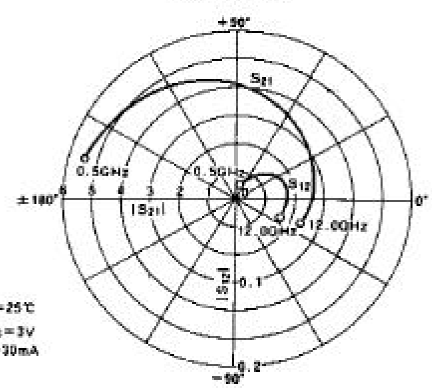

S PARAMETERS (T_a=25°C, V_{DS}=3V, I_D=30mA)

Freq. (GHz)	S_{11} Mag.	S_{11} Ang.	S_{21} Mag.	S_{21} Ang.	S_{12} Mag.	S_{12} Ang.	S_{22} Mag.	S_{22} Ang.	K	MSG/MAG (dB)
0.5	0.995	−16.4	6.393	164.9	0.017	78.7	0.579	−11.4	0.067	25.0
1.0	0.966	−27.1	5.224	155.4	0.022	72.1	0.564	−18.3	0.233	23.8
1.5	0.936	−37.7	5.056	145.8	0.027	65.4	0.549	−25.1	0.350	22.7
2.0	0.906	−48.3	4.858	136.3	0.032	58.8	0.534	−32.0	0.442	21.8
2.5	0.876	−48.9	4.720	126.8	0.037	52.2	0.519	−38.9	0.520	21.1
3.0	0.847	−69.6	7.662	117.3	0.042	45.6	0.504	−45.8	0.589	20.3
3.5	0.817	−80.2	4.363	107.7	0.047	38.9	0.489	−52.6	0.652	19.7
4.0	0.787	−90.8	4.215	98.2	0.052	32.3	0.474	−59.5	0.713	19.1
4.5	0.758	−100.6	4.040	89.7	0.054	27.5	0.461	−66.2	0.800	18.8
5.0	0.729	−110.3	3.865	81.2	0.055	22.6	0.447	−72.9	0.893	18.5
5.5	0.700	−120.1	3.690	72.7	0.056	17.8	0.433	−79.6	0.993	18.2
6.0	0.671	−129.8	3.515	64.2	0.058	12.9	0.420	−86.3	1.101	15.9
6.5	0.652	−137.9	3.378	56.8	0.058	9.4	0.418	−92.5	1.188	15.0
7.0	0.632	−146.0	3.241	49.5	0.058	5.9	0.417	−98.7	1.282	14.3
7.5	0.612	−154.0	3.103	42.1	0.058	2.3	0.416	−104.9	1.386	13.6
8.0	0.593	−162.1	2.966	34.7	0.058	−1.2	0.414	−111.1	1.501	12.9
8.5	0.577	−177.0	2.883	27.8	0.057	−3.4	0.414	−116.3	1.596	12.6
9.0	0.561	175.6	2.799	20.9	0.057	−5.5	0.413	−121.5	1.699	12.0
9.5	0.545	168.1	2.716	14.0	0.057	−7.7	0.413	−126.7	1.810	11.6
10.0	0.529	160.3	2.633	7.1	0.056	−9.8	0.413	−131.9	1.929	11.2
10.5	0.515	152.4	2.571	0.2	0.056	−12.9	0.419	−137.0	1.998	10.9
11.0	0.502	144.6	2.508	−6.8	0.056	−16.0	0.426	−142.1	2.070	10.6
11.5	0.488	136.7	2.446	−13.7	0.056	−19.0	0.433	−147.1	2.145	10.3
12.0	0.475	147.5	2.384	−20.6	0.056	−22.1	0.439	−152.2	2.223	10.1

MITSUBISHI ELECTRIC

MITSUBISHI SEMICONDUCTOR <GaAs FET>

MGF1302

LOW NOISE GaAs FET

NOISE PARAMETERS (V_{DS}=3V, I_D=10mA)

Freq. (GHz)	Γopt. Magn.	Γopt. Angle (deg.)	Rn (Ω)	NFmin. (dB)
1	0.747	5.6	25.7	0.77
2	0.683	22.4	26.3	0.82
3	0.638	42.2	26.9	0.89
4	0.595	63.5	27.5	0.96
5	0.562	80.2	28.1	1.19
6	0.530	97.9	28.7	1.41
7	0.503	115.2	28.3	1.63
8	0.475	134.5	30.0	1.85
9	0.450	150.7	26.3	2.08
10	0.430	167.2	22.6	2.30
11	0.408	−174.5	18.8	2.53
12	0.385	−155.3	15.0	2.76

Glp and P1dB (Ta=25℃, V_D=3V)

	f=4GHz		f=12GHz	
	I_D=10mA	I_D=30mA	I_D=10mA	I_D=30mA
Glp (dB)	15.5	16.8	9.6	10.5
P1dB (dBm)	12.6	14.5	10.5	12.7

2—10

MITSUBISHI ELECTRIC

APPENDIX B

COMPUTER SIMULATION RESULTS

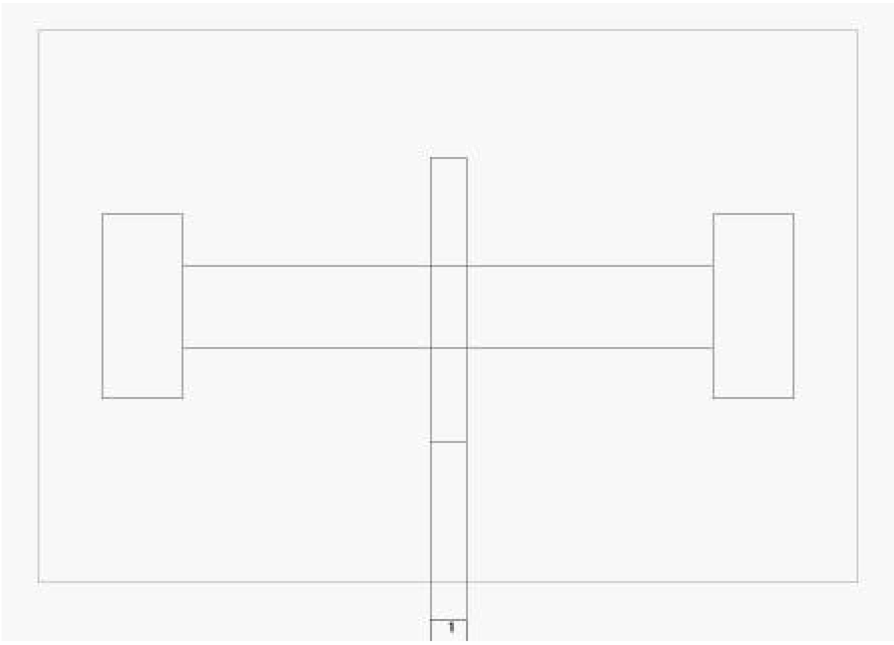

Aperture coupled microstrip antenna layout in *Ensemble*

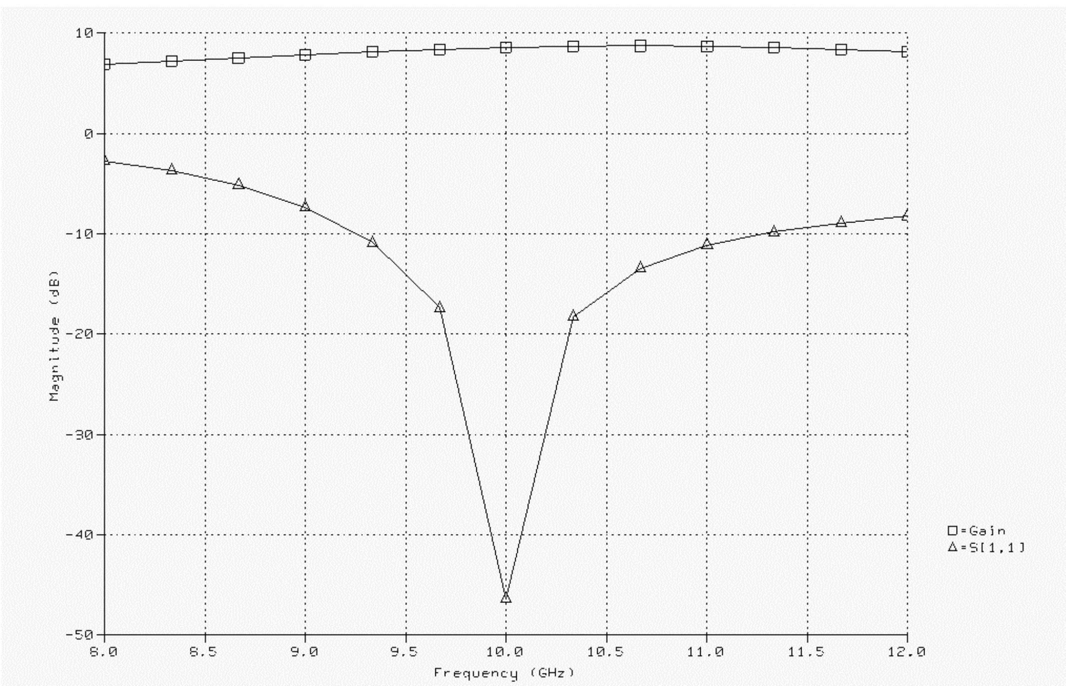

ACMA patch S_{11} input return loss with gain characteristics simulated in *Ensemble*

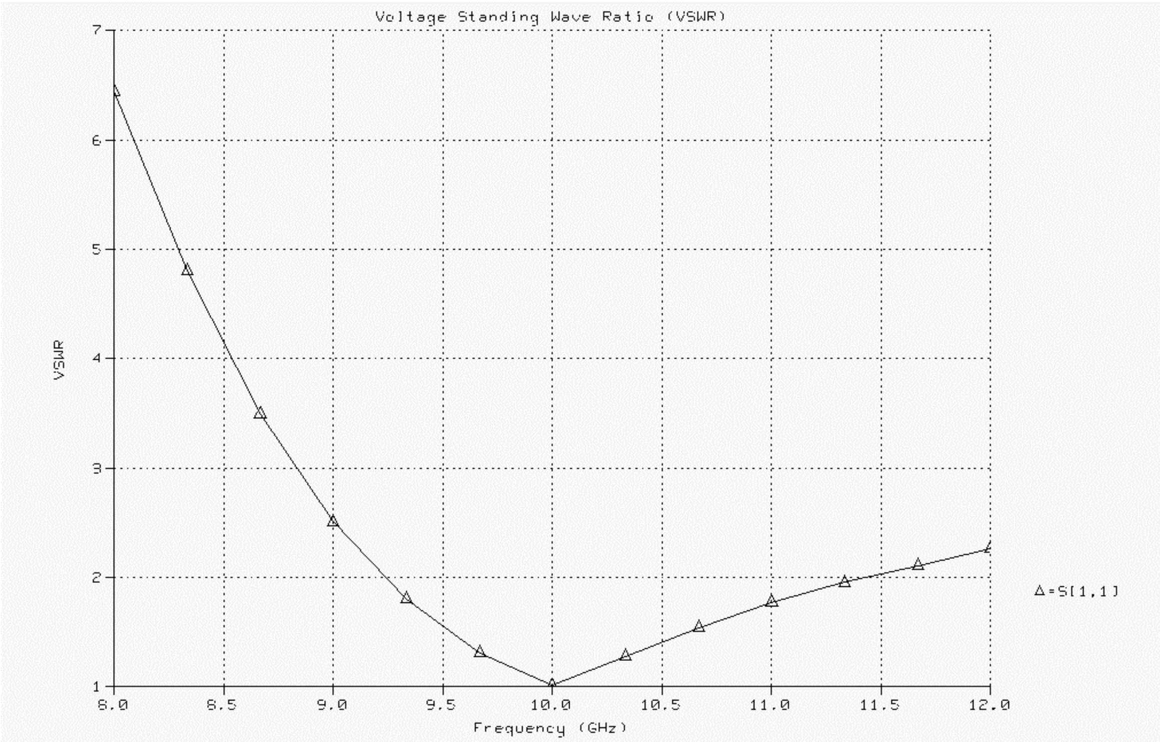

ACMA patch VSWR plot simulated in *Ensemble*

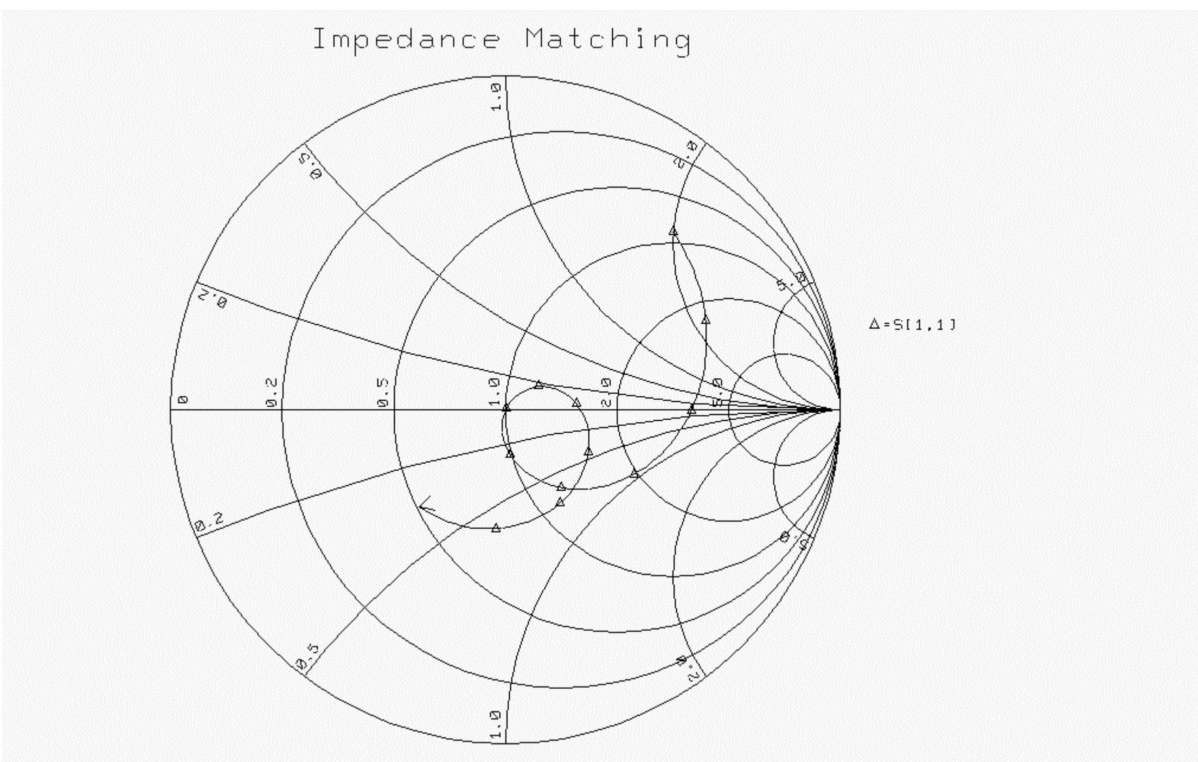

ACMA patch Smith chart showing impedance locus simulated from *Ensemble*

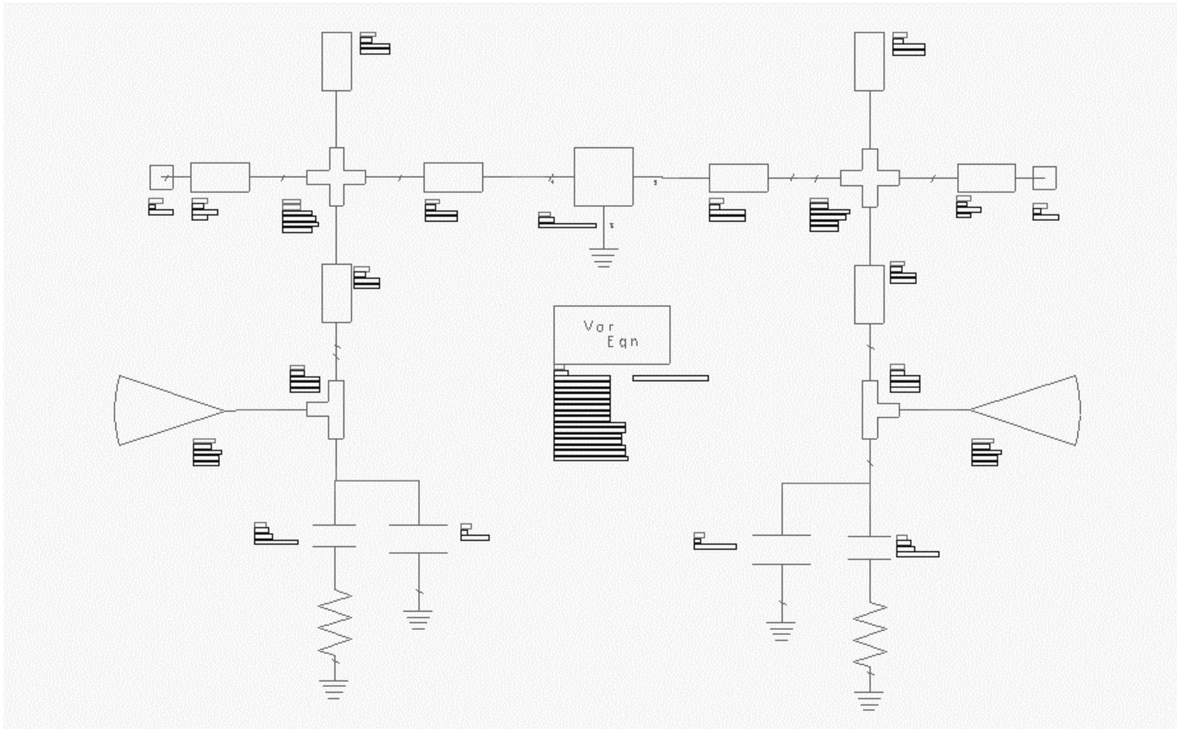

Single active stage transistor amplifier schematics drawn in *Touchstone*

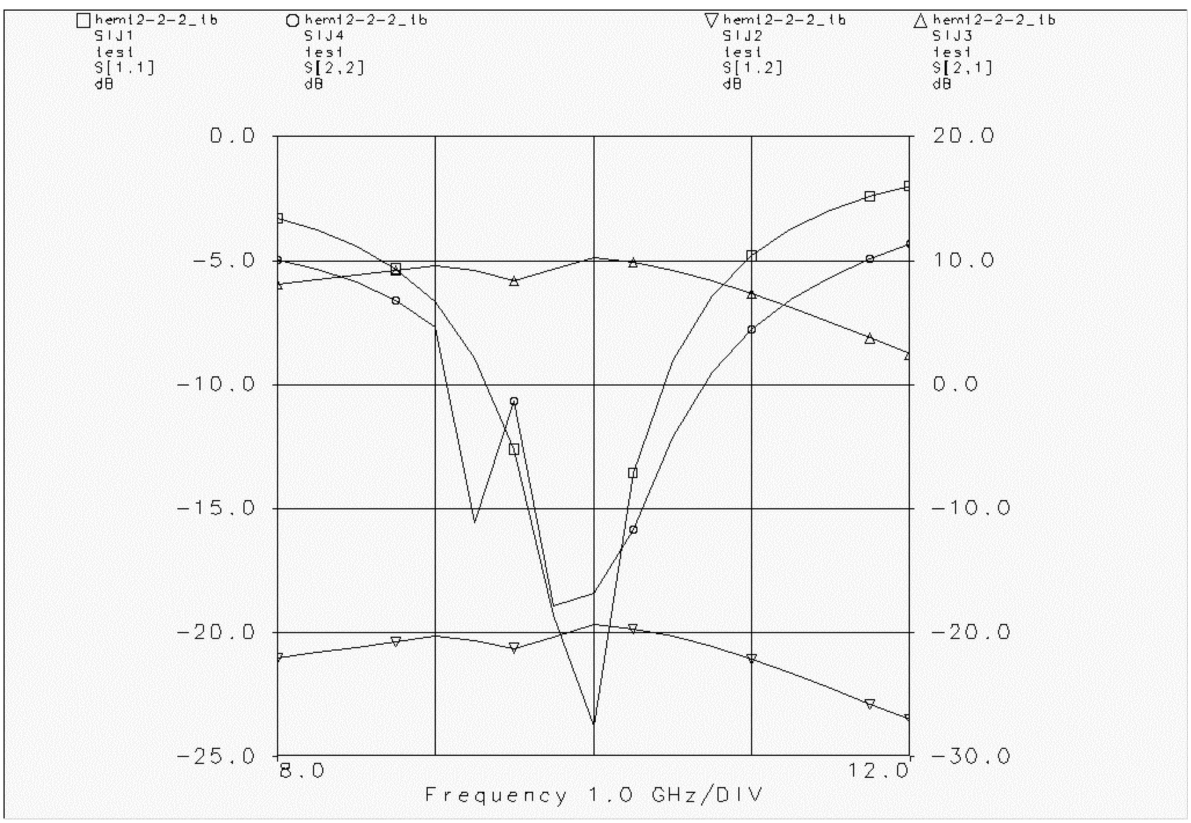

Touchstone S-parameter simulation for single active stage

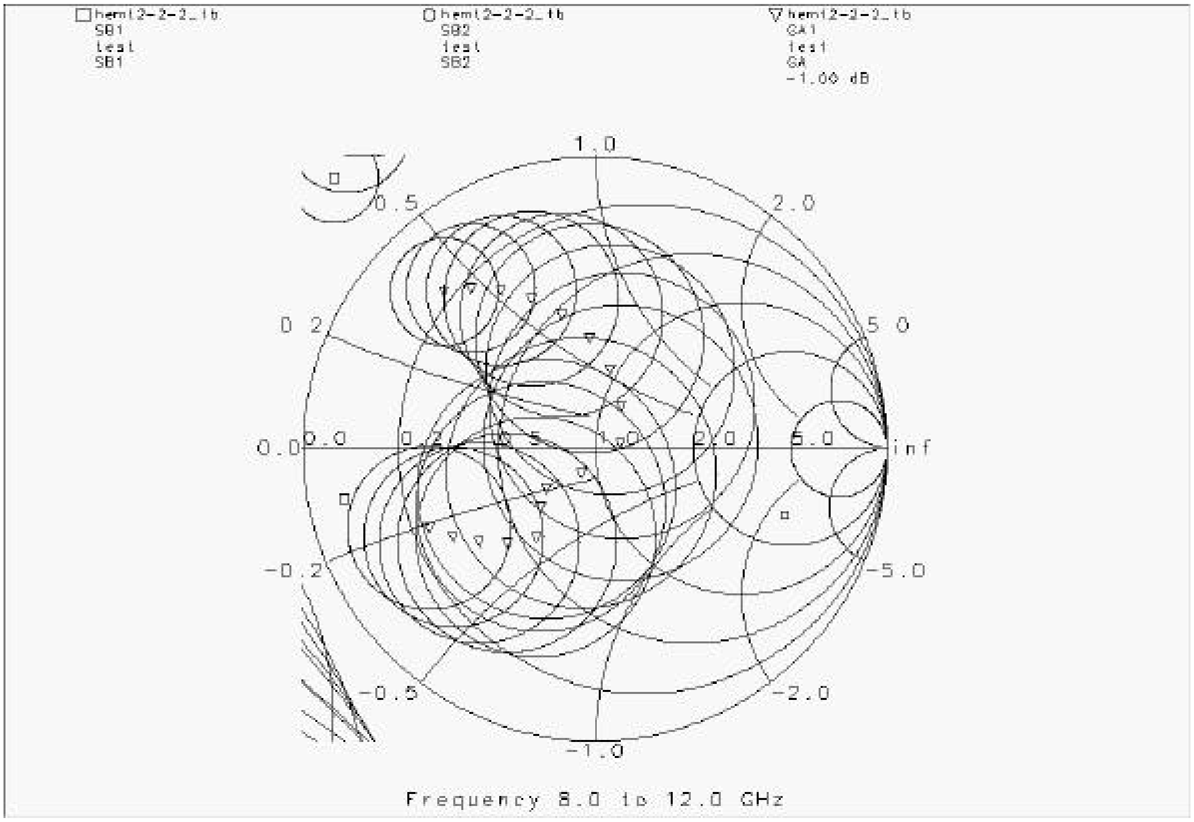

Stability (circles and squares) and Constant Gain (triangles) circles of single active stage simulated in *Touchstone*

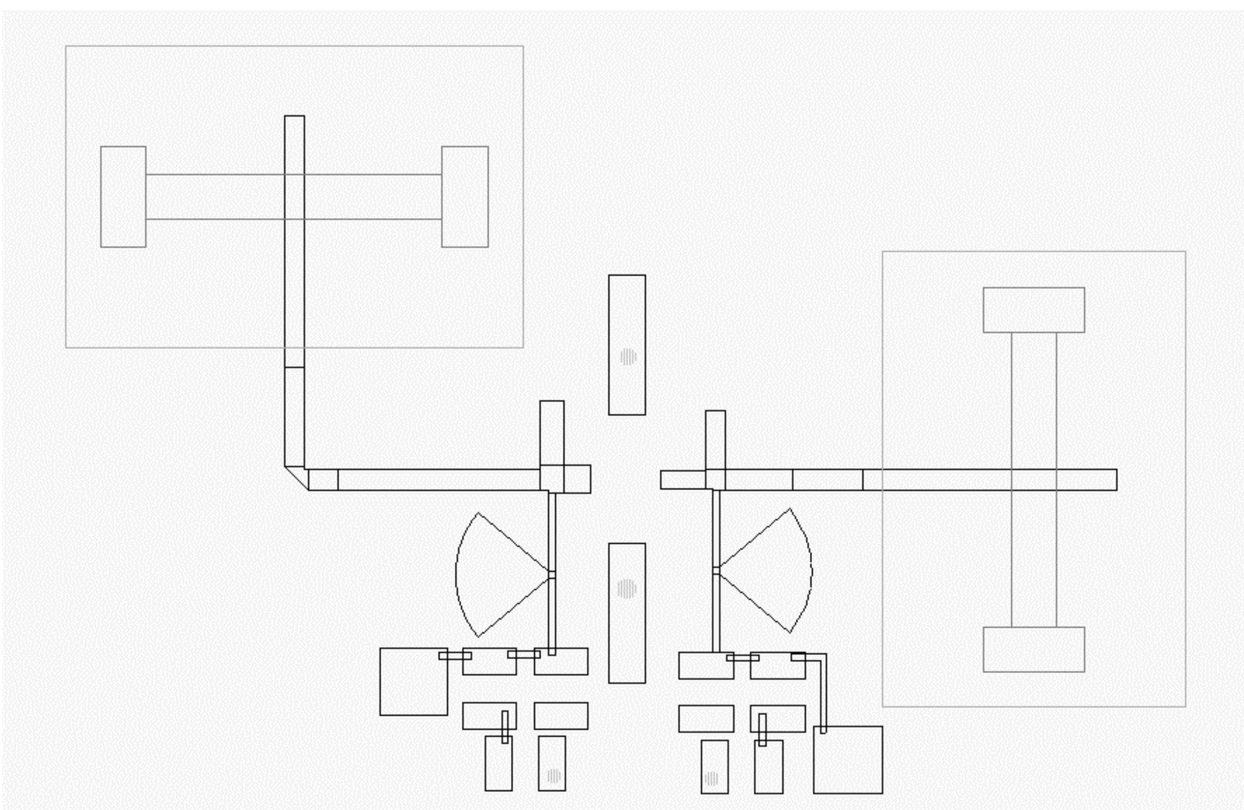

Layout of single quasi-optical unit cell amplifier produced from *Touchstone Layout*

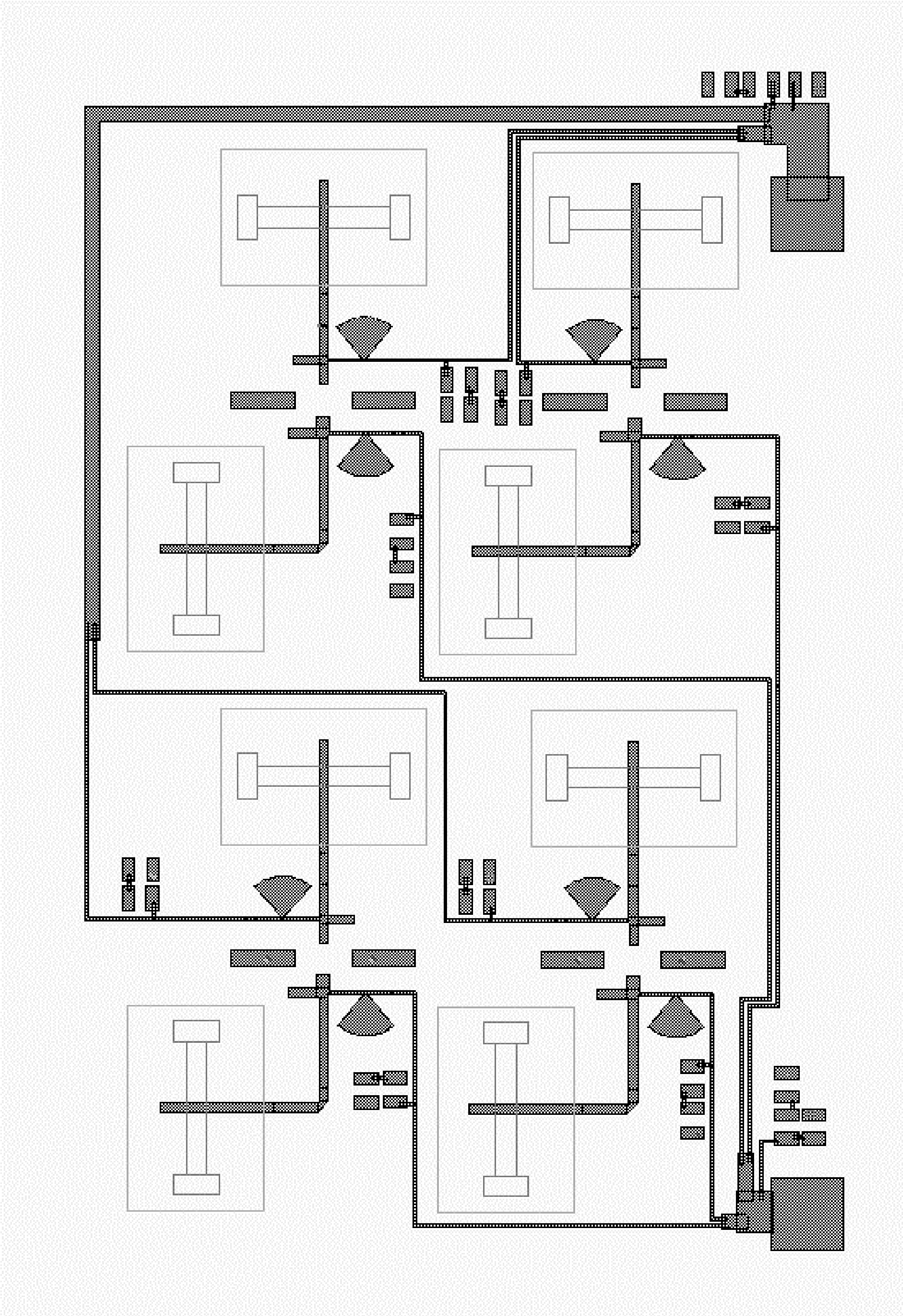

Layout of 2 x 2 4-element array quasi-optical amplifier produced from *Touchstone Layout*

APPENDIX C

EXPERIMENTAL RESULTS

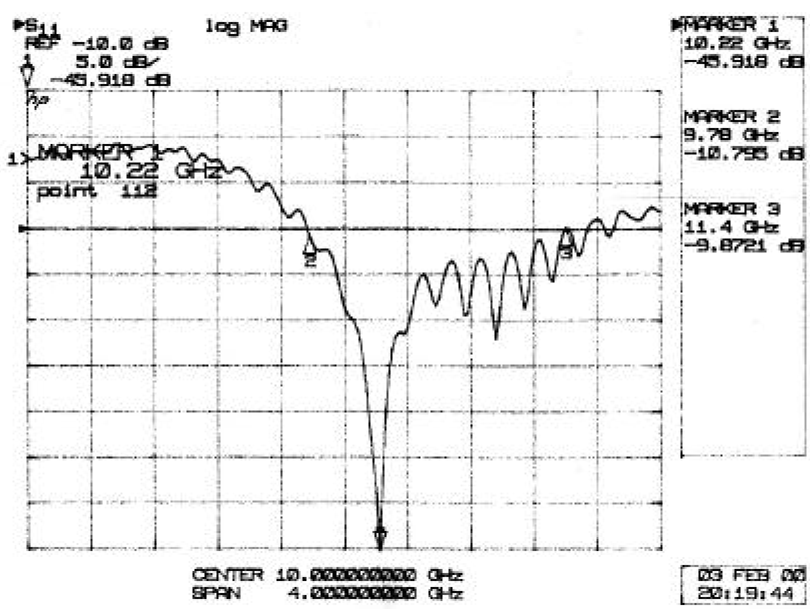

ACMA patch S_{11} input return loss measurement

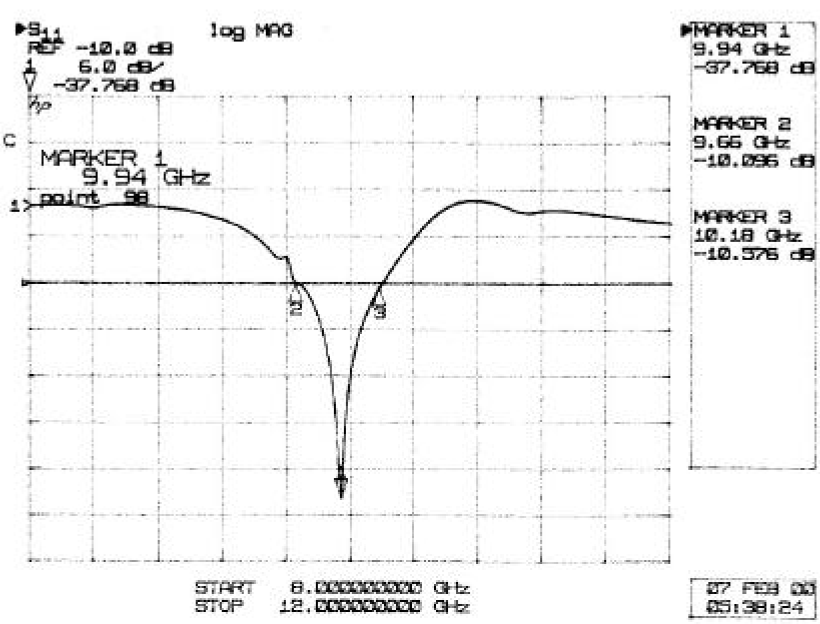

Single active stage S_{11} input return loss measurement

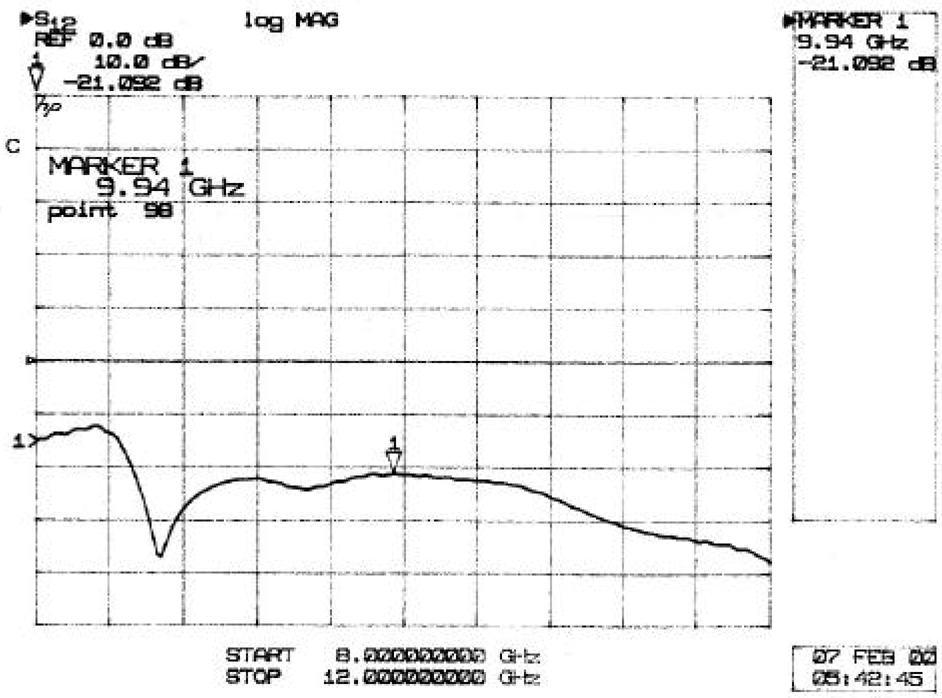

Single active stage S_{12} reverse transmission coefficient (isolation) measurement

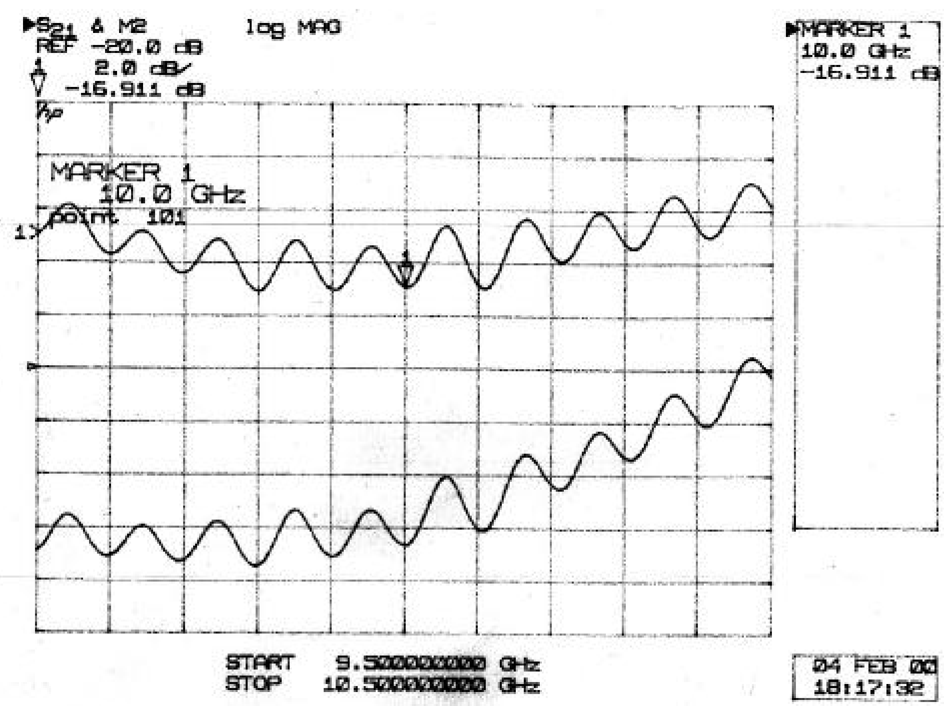

Single active stage S_{21} forward transmission coefficient (gain) measurement

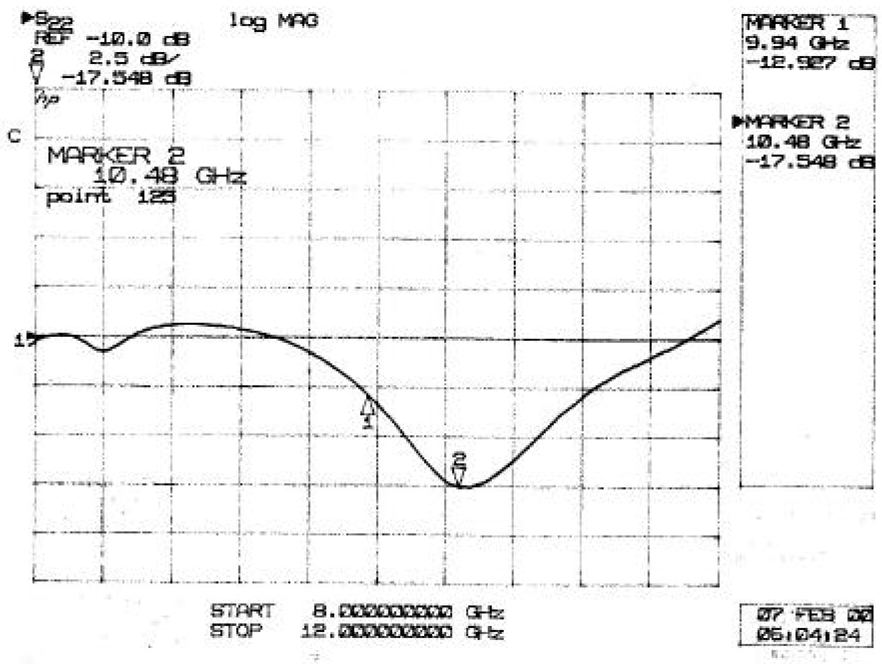

Single active stage S_{22} output return loss measurement

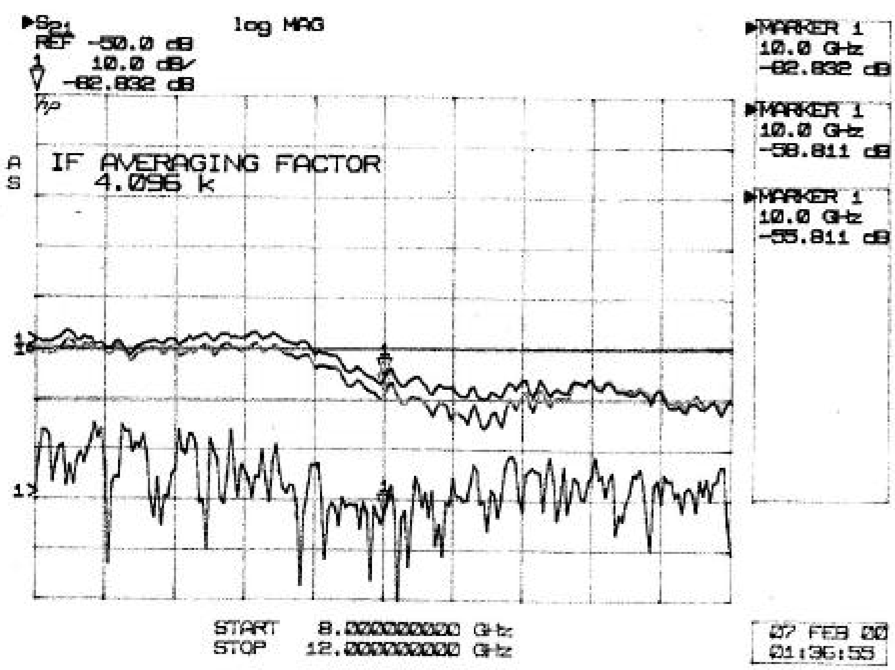

Measured S_{21} gain of 2 x 2 array quasi-optical amplifier with 0, 2, and 4 elements exposed

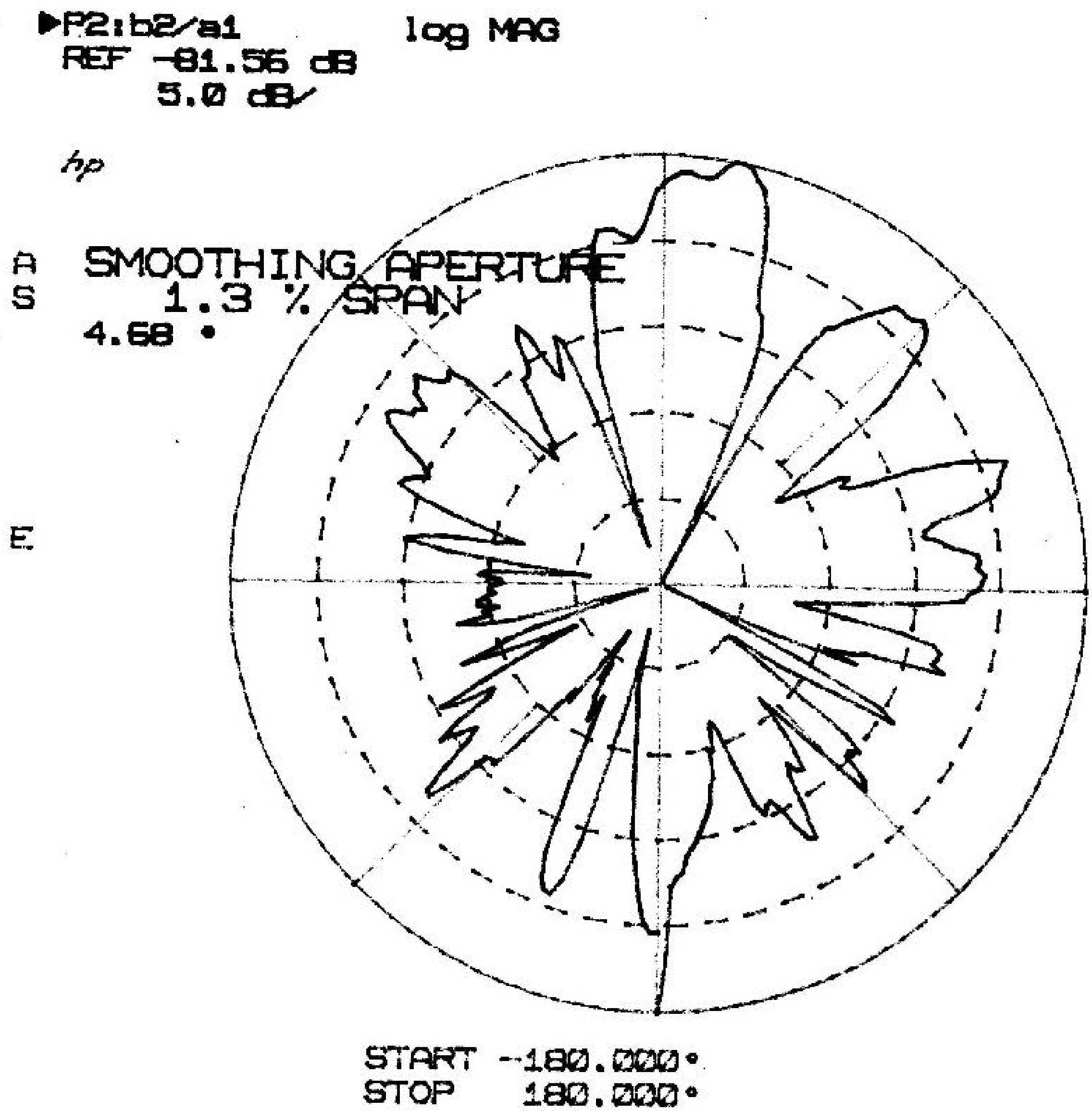

Measured far field radiation pattern for 2 x 2 4-element quasi-optical array amplifier